Multiphase Stirred Tank Bioreactors – New Geometrical Concepts and Scale-up Approaches

Lutz Böhm*, Lena Hohl, Chrysoula Bliatsiou, and Matthias Kraume

DOI: 10.1002/cite.201900165

Mainly with respect to biotechnological cases, current developments in the field of impeller geometries and findings for multistage configurations with a specific view on aerated stirred tanks are reviewed. Although often the first choice, in the given case the 6-straight blade disc turbine is usually not the best option. Furthermore, quantities usable for scale-up, specifically applicable in this field are discussed. Only quantities taking local conditions into account appear to be able to actually compare different stirrer types and scales.

Keywords: Aerated stirred tank, Cultivation, Impeller, Multistage stirrers, Scale-up

Received: October 11, 2019; *accepted:* October 14, 2019

1 Introduction

Asking experts on general rules for the layout of stirred tank reactors, simplified spoken, one will most likely hear about 6-straight blade disc turbines with radial primary flow, also known as Rushton turbines or propellers with axial primary flow. Furthermore, a stirrer diameter d to tank diameter D ratio of $d/D = 0.33$ and a tank with baffles is often used. As a rule-of-thumb, e.g., for a Rushton turbine, a power number N_P (sometimes also called Newton number Ne) of 5 is assumed and a certain power input P per volume V, such as $P/V = 500\ \mathrm{W\ m^{-3}}$, is estimated for a homogenous mixed system at a moderate energy consumption. Specifying the constraints towards a multiphase system, more questions arise such as the number of apparent phases, the density differences between the phases, the desired particle size(s), power input for dispersion or suspension and so on. Once diving deep into the published works (thoroughly combined, e.g., in the Handbook of Industrial Mixing [1], its follow-up [2] and further numerous works of well-known experts in the field), the feeling arises that everything has been investigated and poured into formulas before.

For low disperse phase fractions, it is often assumed that the influence of the disperse phase is neglectable for the overall behavior, especially under turbulent conditions. When it comes to the particle sizes in a stirred tank, a relationship between Kolmogorov length and smallest breaking particle size is drawn repeatedly. To name an example for the commonly used equations, generally accepted and – by many authors – confirmed relations between Sauter mean diameter d_{32} and mean specific energy dissipation rate $\bar{\varepsilon}$ can be condensed for fully developed turbulence in the form $d_{32} \sim \bar{\varepsilon}^{-n}$. The exponent n depends on the fact whether the conditions in the turbulent flow represent the inertial or the dissipation subrange. To apply such correlations, local isotropy of the turbulent flow is assumed. When it comes to the scale-up from laboratory to industrial scale, again experience often leads to rules such as keeping the tip velocity of the stirrer w_{tip} constant due to comparable maximum shear rates apparent in the bulk liquid or using a constant specific power input P/V.

For millennia, stirred tanks were used in small scale for food preparation and for centuries in larger scale applications such as ore extraction. Nowadays, stirred tanks can be found in almost all industrial branches reaching from the chemical to the biotechnological industry including pharmaceutical, cosmetics and food production. The broadening of the application fields also leads to more and more specific constraints and demands. The cultivation of fungi or mammalian cells within aerated stirred tanks, e.g., for the production of enzymes or antibody fragments, can be used as a bold example for the specific needs that necessitate solutions going beyond classical stirrer designs and rule-of-thumb power inputs. Together with advancing possibilities, decreasing prices of additive manufacturing and more and more available advanced materials, this leads to a very broad range of stirrer types, basically covering all types of small high-frequency to large low-frequency impellers. Furthermore, specifically on laboratory scale, certain standards found in chemical industry obviously are not adapted by suppliers of cultivation systems. The stirrer and tank bottom design, the number and positioning of baffles and so on, differ for all laboratory scale systems on the market.

Dr.-Ing. Lutz Böhm, Dr.-Ing. Lena Hohl, Chrysoula Bliatsiou, Prof. Dr.-Ing. Matthias Kraume
lutz.boehm@tu-berlin.de
Technische Universität Berlin, Chair of Chemical and Process Engineering, FH6-1, Straße des 17. Juni 135, 10623 Berlin, Germany.

While in small scale, homogeneous mixing might reasonably be expected in almost all cases, this cannot generally be assumed in large-scale production, which is of high importance especially in a lot of biotechnological applications. The conditions in the aerated stirred tank for the cultivation of microorganisms can cover:

- time-dependent, often non-Newtonian rheological behavior of the cultivation broth in combination with
- shear-sensitive micro-organisms/cells and, at the same time,
- targeting an oxygen transfer rate larger/equal to the oxygen uptake rate while
- having substrate concentration-depending metabolisms with different kinetics for metabolism changes from biomass built-up or production to "survival" mode and back.

This briefly illustrates the complexity of the design task at hand. Again, a general rule-of-thumb might say that low-shear stirrers have comparably high power numbers. However, a real definition of low-shear stirrers does not exist. Nienow [3] gave an overview concerning the important physical aspects such as volumetric mass transfer coefficient k_La, local flow characteristics (shear stress near the stirrer or specific energy dissipation), local and overall homogeneity of the bulk and air-phase mixing, power input, heat transfer or microcarrier suspension. Furthermore, he summarized biological aspects such as growth and productivity, local and overall substrate and CO_2 concentration, pH value, temperature and shear sensitivity. As Pangarkar [4] wrote "Design of stirred bioreactor is fraught with many unknown parameters and could even be classified as a chemical engineer's nightmare. Several constraints are to be satisfied simultaneously and these include very small operating windows. Considerable progress has been made in understanding the causes of damage to cells, in particular the fragile animal cells. The hydrodynamic effects are, however, not adequately studied in real systems and much needs to be investigated in this area."

As orientation, with these conditions for a multiphase stirred tank in mind, this article aims at the following: Sect. 2 will review developments in the field of stirrer designs. Furthermore, in this context, multistage stirrers with different stirrer type combinations will be discussed, as these are of high interest since filling height H to tank diameter ratios $H/D > 1$ become more common in laboratory and industrial scale. A focus will be on possibilities how to predict the behavior of such systems. Here, one of the main aims is discussing the role of computational fluid dynamics (CFD) in the characterization allowing a better understanding going beyond commonly used parameters.

Sect. 3 will review methods to characterize such systems usually related to scale-up criteria. Different approaches reaching from rather global quantities up to quantities considering local information in the system will be discussed and assessed for their applicability.

2 Impellers Used in Cultivation Systems

2.1 Single-Stage Impellers

The variety in the design of stirrers is pretty broad. Due to the nature of the stirred tank setup, even completely new developed stirrers can be categorized into certain already existing groups. One possibility to generally categorize stirrers is sorting the different geometries into near-wall and distant-wall stirrers. A value allowing the sorting of the different types into the two groups is the ratio of the stirrer diameter to the tank diameter. Roughly, values for $d/D > 0.5$ mean that the stirrer is rather a near-wall stirrer. Anchor or helical ribbon impellers are typical examples of this type, while the 6-straight blade disc turbine (6-SBDT), also known as Rushton turbine, and the propeller (PROP) usually fall into the distant-wall group. The stirrers discussed in this section are mostly tested with filling height to tank diameter ratios of $H/D = 1$. Although original research papers dealing with the comparison of different stirrer types can only cover a small number of different impeller types, summarizing works like the Handbook of Industrial Mixing [1] give a broad overview about general and specific knowledge gathered in the field. Therefore, here the aim is rather collecting information about newly developed stirrers and stirring strategies discussed in the years after the publication of the handbook (without neglecting Kresta et. al.'s update [2]; see Tab. 1 for information about the discussed publications with single impellers).

In publications discussing the comparison of the different stirrer types, the 6-SBDT is often used as the default impeller. Due to its combination of the horizontal disc with vertical blades, it is a well-established choice for aerated stirred tanks. Still some experts claim this might not necessarily be the best choice as the default system. It is actually not so easy to characterize its behavior very well. Just to give an example why this can be such a challenging task: usually, the secondary flow field of the 6-SBDT is assumed as being purely radial with two toroidal ring vortices, one above and one below the stirrer. Once the flow field is actually investigated, it becomes clear that the secondary flow field is very sensitive, e.g., to the shape of the bottom (flat or dished bottom), the installation height of the baffles and the clearance height of the stirrer from the bottom. Although usually not expected from the 6-SBDT, with a certain distance of the baffles from the bottom and at a certain ratio of stirrer and tank diameter d/D, the secondary flow field can be become a mixture of a radial and axial (e.g., [5]). This is not surprising, as the 6-SBDT can very well be used as an impeller in stirred tanks with a draft tube at low clearance height resulting in a single loop flow field, typical for axial impellers [6].

2.1.1 Up-Pumping Impellers

Although for most cases usually not an intuitive choice, especially for aerated stirred tanks, Nienow and Bujalski [7]

Table 1. Comparison of studies on single impeller cases regarding approaches and outcome.

Reference	Experimental / numerical	Material system	Impeller types	Setup information	Measured quantities (selection)
up-pumping					
[7]	exp/num	Newtonian / non-Newtonian	3SHPU, A315, B2-45, MFLOWT, LE20		
[8]	exp	Newtonian / air	EED, EEUP	flat bottom, $H/D = 1$	mean specific energy input, flow number, gas holdup
[9]	exp/num	Newtonian / air	6-SBDT, 6-PBU, A310	$V = 9.8$ L, flat bottom, $H/D = 1$	local gas holdup, mixing time
new designs					
[10]	exp	Newtonian liquid / liquid	6-SBDT with different d/D, 6-PB with different angles, PROP with different h/d, PROP-R, BiLOOP, WRIB with different angles	$V = 3.2$ L, dished bottom, $H/D = 1$	power input, Sauter mean diameter
flexible shaft					
[11]	exp/num	cultivation broth (fungi, non-Newtonian) air	FZ, SS	$V = 1.5$ L, flat bottom, $H/D = 1.3$	biological parameters
[12]	exp/num	cultivation broth (fungi, non-Newtonian) air	6-SBDT, SS	$V = 1.5$ L, flat bottom, $H/D = 1.3$	biological parameters, power input, changing rheology, mixing time, k_La
single flexible impeller					
[13]	exp	water	6-SB, 6-CB, 6-SBflex	flat bottom	normal vibration of flexible blades, flow field
[14]	exp	Newtonian / air	6-SBDT, 6-PB, 6-SBDTflex, 6-PBflex	$V = 86$ L, flat bottom, $H/D = 1$	power input, local gas holdup

discussed the benefits of up-pumping impellers, specifically large surface area hydrofoil impellers. Besides the good mixing performance with respect to the dispersion of gas, the up-pumping impellers work very well for the suspension of settling and floating solid particles (also with additional aeration), the homogenization of the liquid phase in multiple phase systems (in multistage reactors) and the distribution of substrate for surface feeding fed-batch systems. Although, an acceleration of the gas bubbles towards the surface along the shaft and, therefore, lower gas holdups and volumetric mass transfer coefficients k_La might be expected, newer publications confirm another trend. For often used axial down-pumping impellers, bubbles are dispersed near the impeller and tend to gather below it, especially with higher rotational speeds [9]. At higher gas flow rates, typically a loading is visible which also results in a decrease of the stirrer power input at the same rotational speed [7].

Zhou et al. [8] investigated elephant-ear impellers in a down-pumping (EED) and up-pumping mode (EEU) and confirmed that for low gas flow rates ($Q_g < 0.05$ vvm; volume of gas per volume of liquid per minute; value typical for mammalian cell cultivation), the power number N_P of neither the EED nor the EEU was affected by the aeration. This is independent of the rotational speed and the EED has consistently higher values of the power number by approximately 25 % in comparison to the EEU. Once increasing the gas flow rate by an order of magnitude ($Q_g = 0.5$ vvm, value typical for bacterial cultivation), in case of the EED the power number decreases by 10 % (for low rotational speeds) up to 40 % (for higher rotational speeds). The power number of the EEU is not affected by the aeration. For higher rotational speeds, N_p is higher by approximately 15 % in comparison to the value of the EED and shows less enhanced torque instabilities.

For higher gas flow rates, Montante and Paglianti [9] compared a 6-SBDT, an axial down-pumping Lightnin A310 (A310) and an up-pumping 6-pitched blade turbine (6-PBU). The measured properties were the local gas holdup, the flow regime and the mixing time. With gas flow rates going above the flooding point, the measurements showed a high mixing effectiveness (characterized by the dimensionless mixing time $\theta = t_{95}N$; mixing time till 95 % homogeneity is reached in the tank t_{95}; rotational speed N) and a more equal gas distribution, especially above the impeller plane in comparison to the down-pumping impeller. Zhu et al. [8] showed experimentally (with the help of

particle image velocimetry; PIV), specifically for the same impeller geometry just in up- and down-pumping mode, that up-pumping impellers display a unique flow field in the tank. Although not discussed in literature yet for single up-pumping impellers in this way, in aerated stirred tanks independent of the gas flow rate this mode leads to a higher number of bubbles passing through the region between the blades and close by the impeller itself. This results in smaller bubbles, in combination with a flow field allowing the more homogeneous distribution of these smaller bubbles in the tank as Montante and Paglianti [9] indicated, especially for the region above the impeller. Although Bliatsiou et al. [10] investigated a non-aerated liquid-liquid system, their results for droplet sizes found for an up-pumping impeller (up-pumping bionic loop impeller; BiLOOP) in comparison to diverse other common impeller geometries underline this assumption.

At the same mass (M) specific power input, or mean energy dissipation rate, $\bar{\varepsilon} = P/M$, smaller Sauter diameters were found for the up-pumping impeller in comparison to the radial flow impellers and the pitched blade (diagonal flow) impellers. Together with the stable power input over a broad range of gas flow rates and the aforementioned ability of a simultaneous suspension of settling and floating solid particles, this shows a high potential of the axial up-pumping impellers in aerated stirred tanks, especially in the field of biotechnological cultivation. To actually understand the mechanisms behind these findings, numerical approaches with CFD appear to be the only valid option to gain local information with a reasonable temporal and spatial resolution as the flow field, specifically for high gas flow rates, cannot be determined experimentally. The promising attempt of Montante and Paglianti [9] of correlating, e.g., experimental data of gas holdup and mixing time with dimensionless numbers including the dispersion coefficient could then be fed with information not obtained by CFD yet.

2.1.2 New Impeller Design Approaches

With additive manufacturing and advanced materials being progressively accessible at moderate prices, new approaches in the field of stirrer system designs are appearing. Some of the approaches tend to specifically tackle the topic of local shear stress appearing in the tank responsible for the non-beneficial influence on biological growth. Others tend to consider the changing rheological characteristics of fermentation broth during cultivation time.

Bliatsiou et al. [10] investigated a broad range of radial and axial impellers. The aforementioned up-pumping impeller and other impellers were inspired by bionic approaches successfully implemented in boat propeller design and as CPU cooling devices. The idea behind these impeller geometries is comparable to the winglet approach established in the airfoil design of planes. The tip region of the impeller is usually the volume with the highest shear appearing in the system and, therefore, crucial for the biological material in the cultivation broth. The winglet approach usually results in a larger surface area of the stirrer and, therefore, a larger area where shear forces can act but, potentially, it leads to more controlled flow behavior at the tip with lower local energy dissipation values. Besides numerous types of 6-SBDTs, down-pumping pitched blade impellers (6-PB) and PROP, a simplified winglet approach with a ring around a propeller (PROP-R, Fig. 1a), the aforementioned BiLOOP (Fig. 1b) and the more abstract implementation in the wave-ribbon geometry (WRIB, developed by EvoLogics GmbH, Fig. 1c,d) were tested. Such geometries can only be produced with reasonable effort and the potential of quickly testing adjusted cases with the help of additive manufacturing. Tests were performed in a liquid-liquid system and drop size distributions were determined. In comparison to the established geometries, the new (down-pumping) geometries needed a much higher power input (by an order of magnitude) to disperse the less dense oil in water but, compared to most stirrer types, had less enhanced tendency for surface air entrainment. In all cases this is clearly due to the peculiar flow field produced by the stirrers. For the PROP-R, this can be explained by changing the axial characteristics of the PROP to a rather diagonal flow below the impeller [10]. The WRIBs show a complex behavior rather comparable with the characteristics of a rotating disc [15]. Still, in comparison to the 6-PBDs and PROPs, at the same $\bar{\varepsilon}$, the PROP-R showed higher values of d_{32} and the WRIBs' results lay below these. This indicates lower values of the local maximum shear stress for the PROP-R and vice versa for the WRIBs.

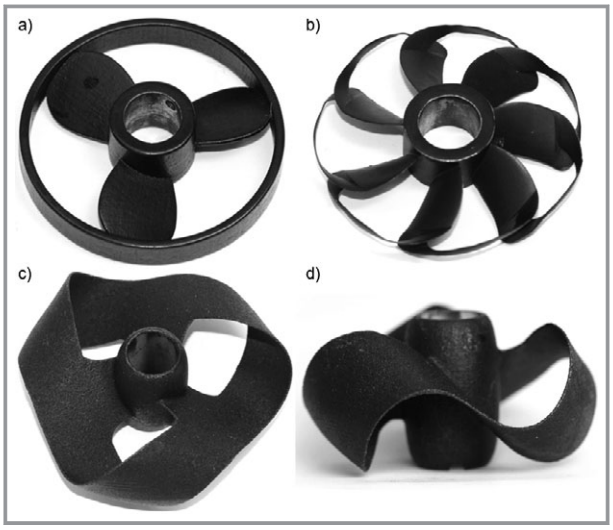

Figure 1. New impeller designs incorporating the winglet approach; a) PROP-R, b) BiLOOP, c) WRIB isometric view (d/D = 0.4), d) WRIB side view (d/D = 0.33) (further described in [10]).

Approaches going beyond $\bar{\varepsilon}$ were applied to correlate d_{32} considering local characteristics such as impeller swept volume V_I (resulting in the energy dissipation circulation function EDCF) [16] or local maximum energy dissipation rate

ε_{max} [15] (further discussed in Sect. 3). Although these approaches considering impeller-specific local data yielded promising first results, the analyzed data also showed the downside of these approaches. Some of the local information incorporated in the correlations are mostly not directly measured but again calculated by correlations, e.g., considering geometrical parameters of the impeller. For completely new impeller designs, these subcorrelations often do not work or cannot be calculated at all. Here again, as first attempts applying CFD proved, local information can be made accessible (results not published yet). For instance, for the WRIB it was found that following the path of a particle through the reactor, the residence time of this particle in the high-shear zone near the impeller is much higher in comparison to that for a 6-SBDT. Other CFD approaches can include specific geometrical optimizations of impeller geometries with respect to the aforementioned local values.

2.1.3 Flexible Impeller Parts

2.1.3.1 Flexible Shaft

Besides the attempt to avoid, e.g., high values of shear stress responsible for the disintegration of microorganisms, by geometrical adjustments of the impeller, one approach considering the potentially changing rheological behavior of the cultivation broth during the fermentation time is using flexible parts in the stirring system. Ghobadi et al. [11, 12] applied the Swingstir® impeller (SS) in their fungus cultivation experiments and compared its performance with a Fullzone® impeller (FZ; large impeller covering the whole filling height just at the lower limit of the near-wall d/D value) and two 6-SBDTs in a multistage arrangement. The SS is an off-center stirrer with a flexible shaft moving concentrically above the aerator. In comparison to the two other centered impeller configurations, the SS proved in the system with a changing shear-thinning behavior a very good performance in terms of high volumetric oxygen transfer rates k_La (also for higher fermentation times and, correspondingly, higher viscosities) and low average shear stress values (lower by an order of magnitude for all fermentation times in comparison to the 6-SBDT). In high viscous liquids, the tendency of a centric gas flow is enhanced. Off-center impellers improve the gas distribution in such reactors. The specific behavior of the SS influenced the rheological changing of the broth over time resulting in lower consistency indices K and flow indices m (Ostwald-de Waele approach: $\mu = K\dot{\gamma}^{m-1}$; with the viscosity μ and the shear rate $\dot{\gamma}$). Following these results, for the specific cultivation tested here, the biological system showed the best performance for the SS in terms of yield production. Although CFD simulations were performed to get a deeper understanding of the overall effect, more work has to be done in this field with multiphase modeling and not only a rotating stirrer but also a flexible shaft.

2.1.3.2 Partly or Fully Flexible Single-Stage Impellers

Besides the flexible shaft, flexible parts of the stirrer itself were recently investigated as well. These developments illustrate, in parts, a parallelism to turbomachinery (e.g., [17–19]) where this idea is picked up as well. For single-impeller non-biological systems, Liang et al. [13] investigated a fully flexible 6-straight blade impeller (6-SBflex) using a specific alloy allowing the desired elasticity while Qiu et al. [14] tested 6-SBDT and a 6-PB with flexible tips made of silicone (6-SBDTflex, 6-PBflex). Both groups compared the flexible impellers with according rigid versions. Liang et al. [13] used two rigid impellers representing the unbend and the most bend (curved) position of the flexible impeller. Regarding N_P, at low rotational speeds the value of the 6-SBflex is between the values of the straight and curved rigid impeller, while, with increasing rotational speed, the power input is up to 10 % higher for the flexible impeller. The higher power input at equal rotational speed is explainable with the flexibility of the stirrer leading to a vibrational movement. In the field of flexible impellers, often turbulence parameters like turbulent kinetic energy (e.g., [13]) or parameters covering chaotic mixing like the largest Lyapunov exponent (LLE, e.g., [14]) are used to characterize the difference to rigid impellers. Such properties can be determined experimentally up to a certain degree of precision but, again, CFD offers a much higher potential regarding temporal and spatial resolution. The specific case investigated experimentally by Liang et al. [13], did not prove to be a valuable choice. The magnitude of velocity fluctuations was influenced by the normal vibration of the blades, but the effect was not strong enough, especially with respect to the higher energy demand for the flexible stirrers. Still, with further development in materials with specific properties and more complex geometries available due to additive manufacturing, in the future, this idea might lead to completely new impeller concepts.

Nonetheless, at the moment, Qiu et al's [14] approach appears to be the more straight-forward option. Adding flexible parts to existing geometries can be realized with a reasonable effort. The work focused on the effect of flexible part variations on the power input and local gas holdup (via conductivity probes) under unaerated and aerated conditions. Depending on the length of the flexible part added to the tip of the impeller, the power number was higher by up to 30 % in comparison to the rigid version of the impeller which can be explained by the additional diameter due to the added flexible parts and, as mentioned before, by the energy uptake due to the flexibility of the tip additions. Their results showed that the chaotic movement represented with the LLE was enhanced for the flexible impellers and regarding the local gas holdup, especially at the same lower rotational speeds, the values gained with the 6-SBDTflex were higher by a factor of two in comparison to the values found for the 6-SBDT. At this stage, in contrast to the flexible shaft investigation discussed before, it is not clear if the enhanced local

fluctuations with flexible impeller parts is beneficial for the cultivation. The strength of these impellers might rather lay in applying lower rotational speeds for reaching comparable mixing and aeration conditions. To get a deeper insight into the mechanisms working here, CFD in combination with finite element methods (FE) might be a reasonable option in the future.

2.2 Multistage Impeller Combinations

While most of the publications discussed before worked with liquid height to tank diameter ratios equal or close to $H/D = 1$, industrial applications in, e.g., biotechnology often work with larger values for this ratio ($H/D = 2–3$) to ensure longer residence time for the provided oxygen through aeration and larger surface to volume ratios for faster heat transfer and better temperature control. In some cases, it is potentially still possible to operate such systems with a single impeller (see, e.g., [20]). In most cases with a biotechnological background, multistage impeller configurations are the standard (see Tab. 2 for information about the discussed publications with multistage impeller configurations).

2.2.1 Radial and Down-Pumping Impellers

In a very fundamental approach, Magelli et al. [22] investigated the power input and mixing time of multistage configurations of 6-SBDTs, 4-pitched blade impeller (4-PB), A310 and Lightnin A315 (A315) and two Chemineer BT-6 (BT-6). The H/D ratio was up to 4 and in all cases the equal impeller type was combined on the shaft with different numbers ranging from two BT-6s up to 12 6-SBDTs. Especially the latter case is up to a certain degree comparable with a Taylor-Couette flow or rotating disc contactors, e.g., used in the field of extraction. Especially with radial flow impellers, such as the 6-SBDT, a strong tendency of compartmentation is apparent in the stirred tank influencing the mixing time and power input. For instance, while the overall power number $N_{P,total}$ increases with the number (J) of 6-SBDTs, for cases with more than two 6-SBDTs the relative power number $N_{P,rel} = N_{P,total}/(JN_{P,1})$ for each impeller decreases by approximately 4 % with each additional impeller stage in comparison to the single-stage case ($N_{P,1}$). It should be noted that the distance between the stages was also a varied property but still this confirmed earlier findings with comparable results (see literature cited in [22]).

Table 2. Overview of discussed publications with multistage impeller combinations.

Reference	Approach	Material system	Multistage impellers (top-down configuration)	Setup information	Measured quantities
general					
[21]	exp	Newtonian liquid / liquid	different combinations of the 2-SB, up to 4: directly above each other (resulting in one larger blade), in line with different distances (same surface area), crossed (same surface area)	V up to 207 L, H/D up to 5	drop size distributions, mixing time, power input
[22]	exp	Newtonian	- up to 12 6-SBDT - up to 4 4-PB - up to 3 A310 - up to 3 A315 - BT-6 – BT-6	flat bottom, H/D =2, 3, 4	mixing time
cultivation					
[23]	exp/num	cultivation broth (bacteria), air	- PROP – PROP – 6-CBDT - 6-ABDT – 6-ABDT – 6-CBDT - 6-ABDT – 6-ABDT – 6-ABDT	V = 35 L, H/D = 1.48	biological parameters, mixing time, shear environment, k_La
[24]	exp	cultivation broth (fungi, non-Newtonian), air	- 6-SBDT – 6-SBDT - 3-PB – 3-PB - 6-SBDT – 3-PB - 3-PB – 6-SBDT	V = 5 L	biological parameters
[25]	exp/num	cultivation broth (fungi, non-Newtonian), air	- 6-SBDT – 6-SBDT – 6-SBDT – 6-SBDT - A315 – A315 – HDY675 – BT-6	V = 12 000 L, H/D = 2.75	O_2, T, pH, OUR, biological parameters
[26]	exp	cultivation broth (fungi, shear thinning), air	- 6-SBDT – 6-SBDT - 6-SBDT – CD-6 - CD-6 – 6-SBDT - CD-6 – CD-6	V = 2 L	k_La
[27]	exp/num	cultivation broth (fungi, non-Newtonian), air	- 6-SBDT – 6-SBDT – 6-ABDT - 6-SBDT – PROP – 6-SBDT - 6-SBDT – 6-ABDT – 6-SBDT	V = 10 L, H/D = 1.71	biological parameters, gas holdup

Table 2. Continued.

Reference	Approach	Material system	Multistage impellers (top-down configuration)	Setup information	Measured quantities
[28]	exp	cultivation broth (fungi, non-Newtonian), air	- small reactor: single - large reactor: 3-HYDRO – 3-HYDRO – one high power number impeller (no further information)	V = 2.5 L, 80 000 L, 130 000 L	biological parameters
up-pumping					
[29]	exp	Newtonian / air	- 6-SBDT - 6-SBDT - 6-SBDT - 3-HYDRO-U – 3-HYDRO-U – 6-CBDT - 6-SBDT – 6-SBDT – 6-SBDT – 6-SBDT - 4-HYDRO-U – 4-HYDRO-U - 4-HYDRO-U – 6-CBDT	V = 12 000 L, 30 000 L	mixing time, power input, gas holdup, flow field
[30]	exp	Newtonian/non-Newtonian / air	- 6-SBDT – 6-SBDT - EED – EEU	V = 4 L	average shear rate, gas holdup, k_La
[31]	exp	non-Newtonian / air	- 6-SBDT – 6-SBDT – 6-SBDT - 3-HYDRO – 3-HYDRO - CD-6 - 3-HYDRO-U – 3-HYDRO-U – CD-6 - IMIG – IMIG – CD-6 - GI – EI - DHR – CD-6	V = 35 L, H/D = 1.48	power input, k_La
[32]	exp/num	cultivation broth (fungi, non-Newtonian), air	- 6-SBDT – 6-SBDT – 6-SBDT - 3-HYDRO-U – 3-HYDRO-U – 3-HYDRO-U	V = 35 L	power input, k_La
[33]	exp	Newtonian/non-Newtonian / air	- 6-SBDT – 6-SBDT - EED – EEU - EEU – EED - 6-SBDR – EED - 6-SBDT – EEU - EED – 6-SBDT - EEU – 6-SBDT	V = 4 L, H/D = 1,71	power input, k_La
[34]	exp	biogas broth (non-Newtonian), air	- 6-SBDT – 6-SBDT - EED – EEU - 6-SBDT – EEU - EED – 6-SBDT	V = 3 L, semispherical bottom	biological parameters, power input
flexible impellers					
[35]	exp	Newtonian liquid / liquid	6-SBDT-6-SBDT-flex	mixer-settler-system, square vessel	LLE, Kolmogorov entropy
[36]	exp/num	Newtonian / solid particles	- 6-PB - 6-PB - 6-PBflex - 6-PBflex - 6-PBflexP - 6-PBflexP	V = 300 L, flat bottom, H/D = 1.66	solid concentration over height
[37]	exp/num	Newtonian / solid particles	- 6-SBDT - 6-PB - 6-SBDT-6PB-flex - 6-SBDT-6PB-flexP	V = 300 L, flat bottom, H/D = 1.66, chaotic motor	LLE, solid concentration over height
large low-frequency impellers					
[38]	exp/num	cultivation broth (fungi, non-Newtonian), air	- 6-SBDT - 6-SBDT - MB (single)	V = 1.5 L, flat bottom, H/D = 1.3	biological parameters
[39]	exp/num	cultivation broth (fungi, non-Newtonian), air	- 6-SBDT - 6-SBDT - FZ (single)	V = 1.5 L, flat bottom, H/D = 1.3	biological parameters

The relative power number decreases with the number of stages once the flow field with one separate compartment per impeller stage is observed. Due to the decreasing distance between the impellers, the interaction between the compartments is enhanced.

Regarding the mixing time t_{95}, Magelli et al. [22] showed existing correlations do not work in predicting this property. In their proposed approach, an idea was chosen, which is comparable to the earlier mentioned backmixing ability (or dispersion coefficient) and also the swept volume approach. The developed correlation works fairly well for the different combinations of the radial 6-SBDT. Also, data could be correlated up to a certain degree for all impeller types in combination with the pumping efficiency [40]. Still, the fluid dynamic conditions for the multistage combinations were highly simplified here and the discussed correlation did not prove to work for all combinations tested.

CFD simulations are a possibility to get a better understanding of the actual size and (especially for non-radial impellers) shape of the compartments and their interaction. For a liquid-liquid system, Maaß et al. [21] tested different combinations of 2-straight blade impellers (2-SB). Among other things, this work carved out the influence of different arrangements of the 2-SBs (in line, perpendicular to each other, crossed in one plane, with different distances between the stages) while keeping the number of impellers constant. Due to this approach, the total impeller surface in the tank is constant. By comparing, e.g., basically one impeller, consisting of four in line 2-SBs directly stacked up on each other, and four perpendicularly arranged 2-SB with a certain distance to each other, it becomes obvious that for the latter case the power number and mixing time is significantly lower (both roughly by a factor of 2). It might be obvious that these properties do not only depend on power input per impeller surface area. Still, this work nicely separates the influence of impeller surface area and actual geometrical arrangement of the impeller within the tank volume. To model particle size distributions with the help of population balance equations (PBE), they used a two-zone model, which was developed for a single-stage system and is fairly common in this field [41]. Instead of actual flow compartments, this approach rather differentiates, although in the original approach fairly rough, between regions of high and low energy dissipation and the region's interaction. While the final values of the modeled Sauter mean diameters fit fairly well to experimental values, the transient behavior could not properly be described. Furthermore, in their case, scale-up with common approaches did not work very well in this multiphase system with multiple impellers. Both results indicate again that the actual flow field within the multistage stirred tank needs to be understood much better, e.g., to be able to predict transient particle size distributions and to come up with working scale-up rules.

Investigations of multistage configurations of radial (6-SBDT, BT-6, 4-straight blade disc turbine 4-SBDT, 6-curved blade disc turbine 6-CBDT, 6-arrowy blade disc turbine 6-ABDT, Smith turbine half pipe blades HDY675, hollow-type six-bladed concave disk turbine CD-6, and centripetal turbine CEPET) and down-pumping impellers (PROP, A315, 3-pitched blade impeller 3-PB, 3-blade hydrofoil impeller 3-HYDRO, and profiled triblade TRIB) in cultivation broth can be found with reactor liquid volumes reaching from V = 2–5 L [24, 26] over V = 10–35 L [23, 27] and up to V = 12–130 m^3 [25, 28]. With the exception of Xia et al. [23] who cultivated bacteria, in all other cases, the cultivation of fungi was investigated. Accordingly, aerated stirred tanks with mostly non-Newtonian continuous phases were apparent here and all groups analyzed biological parameters of the cultivation while Xia, Yang and Zhao et al. [23, 25, 27] additionally performed CFD simulations for their systems. For the fungi cultivation cases, besides the cultivation medium and the air, with the discrete fungi agglomerations a third phase is apparent in the system. As mentioned before, the demands for such a case are broad and in parts counteracting. A brief discussion of the results of the studies is given in the following part.

For the cultivation medium, also in fed-batch cases with substrate added during the cultivation, a homogeneous distribution of all components is necessary. This would rather lead to higher rotational speeds and, specifically in multistage configurations, to the attempt to avoid compartmentation. Still, a combination of 6-SBDTs seems to be the standard, especially in lab-scale fermentation. In the mentioned fed-batch cases, this also enhances the importance of where to actually feed the substrate into the reactor as the feeding position will influence the time of distribution in the system. Besides the compartmentation tendency discussed so far mostly for Newtonian fluids, where a certain volume exchange takes place between the compartments, it should be mentioned that in non-Newtonian cases, especially in viscoelastic cases, flow compartments can appear with almost no exchange with the surrounding fluid [42].

For the air supply, the most important requirement is that the oxygen transfer rate (OTR, represented by the overall k_La of the reactor) is larger than the oxygen uptake rate (OUR) by the microorganisms due to their metabolism. The k_La depends on multiple parameters, e.g., higher rotational speeds lead to a more homogeneous distribution of the bubbles within the reactor and overall smaller bubbles due to higher local shear in the bulk. While the compartmentation has the same negative effect on the homogeneous distribution of oxygen in the system, it can have a positive effect on the overall k_La as the residence time of the bubbles and, therefore, the area for the mass transfer can be increased.

For the fungi phase, to guarantee a supply of substrates to the agglomerates, the minimal requirement is the suspension of the agglomerates within the reactor. Still, the shear sensitivity demands rotational speeds as low as possible. The shear stress not only affects the viability of the microorganisms but also, in case of the fungi, the type of growth, e.g., in rather loose mycelial lumps or rather dense pellets.

Xia et al. [23] found that a combination of axial and radial impellers (top to bottom: PROP, PROP, 6-CBDT) was very beneficial for the overall cultivation process. In comparison to the combinations of only radial flow impellers, mixing time was reduced, shear stress in the system was less enhanced and the overall k_La had the highest value. All of

these physical results reflected in a positive effect on the biological parameters. Two interesting facts can be drawn from the work: for the overall system, the impeller combination resulting in the best biological performance could be correlated to the lowest value of the *EDCF* (further discussed later in Sect. 3). Still, this characterizing value could only be calculated with the help of CFD (with assumptions, e.g., Hardy et al. [28] calculated the value based on the mixing time). As the second fact, the CFD simulations showed that for the tested radial flow impellers the appearing shear near the impeller is independent of the mounting position in the multistage configuration. For the axial flow impellers, the mounting position within the multistage configuration does have an influence. This is a clear conclusion as it underlines the separated nature of the compartments for radial flow impellers in contrast to the combined flow fields of axial flow impellers.

Both facts are only accessible due to the performed CFD simulations. Cai et al. [24] confirmed the beneficial effect on the biological performance when an axial flow impeller (upper position) is combined with a radial flow impeller (lower position). This combination showed better performances in comparison to combinations of two radial flow or two axial flow impellers and also in comparison to an axial/radial flow combination with the radial flow impeller in the top position. Besides the inferior performance with a radial flow impeller in the bottom position, Zhao et al. [27] showed for a combination of three impellers that an impeller combination with only one axial flow impeller in the middle position is also not favorable. Yang et al. [25] illustrate the complexity of the overall topic in biological systems. In the industrial scale case, the cultivation performance of a standard combination of 6-SBDTs was compared to a combination of two axial flow impellers on the top and two radial flow impellers in the bottom position. While cell growth and oxygen uptake rate by the microorganisms was not affected by the impeller combination, the morphology and, therefore, also productivity was positively affected. The concept here also included an adjustment of rotational speed and aeration rate based on dissolved oxygen. Especially notable for industrial scale, while having a positive effect on the biological performance, the power input was significantly reduced by using the axial/radial impeller combination. While Yang et al. [25] adjusted, e.g., the rotational speed during cultivation, most other works are not doing this. Suhaili et al. [26] showed again in their work that the prevailing conditions in the system, specifically the rheological behavior of the cultivation broth, significantly influence which impeller combination shows the best performance at specific points in time. While differences in, e.g., k_La might not be strongly enhanced by a certain impeller combination in the beginning of the cultivation, a significant difference might be visible towards the end. Therefore, an adjustment of the rotational speed might be one possibility, or at constant rotational speed, the best impeller combination for the overall performance over time needs to be chosen. But still, for the latter case, the change of the rheology over time needs to be known which in itself depends again on the chosen impeller combination resulting in different shear fields within the tank.

2.2.2 Combinations with Up-Pumping Impellers

Comparable to the aforementioned studies, for the cases investigating impeller combinations including up-pumping impellers, the reactor liquid volume ranges from $V = 3–4$ L [30, 33, 34] over $V = 35$ L [31, 32] up to $V = 30\ m^3$ [29]. The up-pumping impellers are 3- and 4-bladed hydrofoils (3-HYDRO-U, 4-HYDRO-U) and the aforementioned EEU while the down-pumping axial flow impellers were the 3-HYDRO or EED. In all studies, at least one combination of two or three 6-SBDTs was the default system for comparison and all worked with aeration of a non-Newtonian bulk liquid (except of [29]). In agreement to the earlier presented results, in all cases the combinations with an axial flow impeller mounted in the top position showed the best results in terms of mixing time, k_La and power consumption.

Tang et al. [32] actually showed the positive effect of three 3-HYDRO-U on the overall biological performance. While it is worth mentioning that the (top-bottom) EEU-EED combination showed the best performance in terms of k_La relative to power input [33], in three studies [30, 33, 34] the combination EED-EEU actually showed the best performance in terms of k_La itself. The overall good performance of the impeller combinations with axial flow impellers is mostly correlated to a more uniform flow field and a lower tendency of compartmentation. Specifically, this leads to lower average shear rates, and according to the shear-thinning nature of the liquid, to more uniform distribution of the values of apparent viscosity. While only Tang et al. [32] actually performed CFD simulations in the system and calculated the shear field, all experimental approaches rely on a correlation for the average shear in the system calculated with the help of k_La results. Based on an approach correlating shear and heat transfer in a non-Newtonian system in bubble columns [43], Cerri et al. [44] developed the correlation between k_La and the shear rates which Campesi et al. [45] transferred to the case of an aerated stirred tank. While the correlation incorporates operational parameters (rotational speed and aeration rate) and liquid properties (viscosity or in case of non-Newtonian liquids, K and m), the volumetric oxygen transfer rate k_La is influenced by numerous factors itself. The correlation with factors and exponents specifically to be determined for each setup cannot easily be interpreted but still this method while giving a good rough overview breaks down a lot of influencing factors into an equation not incorporating all of them. For instance, higher shear values might generate smaller bubbles with a large surface area but due to the flow field their residence time might be low. On the other side, lower shear values might generate larger bubbles, which might be trapped in the compartments of a multistage system with radial flow

impellers. It has to be accepted that, at the moment, no experimental method is available to measure locally the shear rates in this aerated system (without influencing the flow field). Therefore, keeping in mind all the complications with multiphase modeling in non-Newtonian liquids, the numerical approach with CFD will still most likely be the only way to actually access local information on shear within this system and, therefore, understand the influence of local shear on the biological performance.

2.2.3 Flexible Single/Multistage Hybrid-Type Impellers

Liu and Gu et al. [35–37] investigated flexible impellers. While Gu et al. [36] investigated two separate impellers with flexible parts in one multistage combination, the same group [37] and Liu et al. [35] connected the two stages with a flexible part turning the multistage combination rather into one large impeller. Gu et al. [37] even coupled the system with a so-called chaotic motor.

Gu et al. [36] used the same 6-PBflex impellers already discussed for the single-stage case by Qiu et al. [14], which were normal 6-PBs with flexible tips made of silicone. The comparison was made for two-stage impeller combinations of two 6-PBs, two 6-PBflex and also of two 6-pitched blade impellers with flexible additions where the rigid parts of the blade were punctured (6-PBflexP). The focus here was on power input and the distribution of suspended solid particles within the reactor. Overall, the combination of two 6-PBflexP showed the best performance in suspending particles due to the jet flow related to holes in the stirrer.

Liu et al. [35] connected the blades of two 6-SBDT with flexible straps while Gu et al. [37] connected a combination of a (top-bottom) 6-PB and a 6-SBDT with flexible and punctured flexible straps. Additionally, Gu et al. [37] tested the system with a so-called chaotic motor which shows time-varying rotational speeds. Actually, the rotational speed was not only time-varying but also included a change of the rotation direction leading to stirring phases in which the 6-PB was actually a 6-PBU. Overall, the chaotic mixing (e.g., quantifiable with the aforementioned LLE) was enhanced while the power numbers were, as could have been expected, significantly higher in comparison to the non-connected impeller combination (by a factor of 5).

Regarding the application in cultivation cases, the same statements made before for the study by Qiu et al. [14] of flexible impellers also hold here for all three mentioned studies as Liu et al. [35] worked in a liquid-liquid and Gu et al. [36, 37] worked in a liquid-solid systems. Therefore, no aeration and no biological conditions were tested.

2.2.4 Near-Wall Stirrers

As with Liu and Gu et al. [35, 37] large impellers were already discussed in a first way, Ghobadi and Xie et al. [31, 38, 39] are worth mentioning as well, comparing the performance of rigid large impellers with combinations of 6-SBDTs. In these three studies, aeration of non-Newtonian liquids was investigated while Ghobadi et al. [38, 39] specifically studied cultivations. Xie et al. [31] was already mentioned for the comparison of multiple impeller combinations. The investigated large impellers (gate impeller GI, ellipse impeller EI, double helical ribbon impeller DHR) were also tested in combinations with GI-EI and the DHR with a radial flow impeller below it. Especially for the case with the DHR, under all tested conditions the k_La showed the lowest value and the negative tendency was even worse with stronger non-Newtonian characteristics of the bulk phase.

Ghobadi et al. [38, 39] compared two large low-frequency impellers (Maxblend®, MB, FZ) with a combination of two 6-SBDTs. In both cases, at comparable P/V a more homogeneous bulk phase with good fungi suspension and k_La was found for the large impellers, while the MB showed higher average shear values in comparison to the two 6-SBDTs. The FZ had lower maximum shear values resulting in a worse biological performance in the first and better biological performance in the second case.

2.3 Generalizable Aspects for Impellers Used in Cultivation

The diverse publications discussed up to here showed a few generalizable aspects.

1) In almost all cases, the 6-SBDT or combinations of it were chosen as the default system.
2) In almost all cases, this default system performed worse with respect to the measured quantities (e.g., biological parameters, k_La, mixing time) than the other tested geometries.
3) For a better performance, the compartmentation tendency of the 6-SBDT needs to be disturbed or avoided at all.
4) EDCF proved to be of high interest in cultivations as best biological performance was found for low values of this quantity. The *EDCF* will be discussed further in Sect. 3.
5) Using CFD for the analysis of the flow field regarding compartmentation and, specifically, the overall and local shear is a helpful tool, also for understanding the biological performance. Regarding the calculation of, e.g., *EDCF*, it is absolute necessary for new impeller geometries and impeller combinations to do CFD simulations to be able to calculate the value.

3 Scale-up Approaches

3.1 Scale-up of Biological Systems in Stirred Tank Systems

Scale-up of stirred tanks especially with high scale-up factors and corresponding large differences in geometrical

characteristics in lab and industrial scale is usually difficult to obtain with complete geometrical and process similarity. Fig. 2 (left) shows how the relation of specific power input between both scales changes with rising scale-up factor for different scale-up criteria. Even with only one scale-up criterion this can easily lead to unrealistic values for application in reality (e.g., extremely high specific power input or agitation speeds). If similarity is desired for several process characteristics, a reliable scale-up with complete similarity is impossible to realize. An often-used compromise is to keep the specific energy input P/V constant (Fig. 2, right). However, knowledge of corresponding correlations for the other process characteristics is necessary or they need to be estimated for realistic scale-up.

Especially in complex biological systems, numerous scale-up parameters can be applied. A list and discussion for fermentation systems is given in [46]. The question arises if the geometry of the tank can be varied to achieve the best process conditions. An example would be to use several feed points for substrates or oxygen to compensate longer mixing times in the industrial scale. Partial similarity is used in most cases so that knowledge of crucial process characteristics is of importance to estimate the effects of it on the process.

Hempel [47] summarized several examples where scale-up was successful after the relevant process parameters were identified. In penicillin production, a constant OTR is the limiting step of the reaction so that mass transfer at the gas-liquid interface needs to be identified. Hence, a scale-up criterion of constant k_La values was used successfully in the 1950s for scale-up over more than four orders of magnitude. This was achieved by keeping a constant superficial gas velocity at a specific energy input. Another historic example with scale-up based on OTR is the production of baker yeast [47]. In case of Vitamin B12 production, however, the k_La criterion often leads to an overestimation of power input on industrial scale. This is caused by different driving forces (concentration differences) at the different scales. At constant k_La, the oxygen intake is higher in industrial scale compared to lab scale due to the higher hydrostatic pressure increasing the driving force. On the other hand, the residence time of air bubbles often is longer in industrial scale so that oxygen depletion can occur and reduce the aforementioned positive effect. These interactions are complex and depend on geometry and process parameters [47].

The criterion of similar tip speed w_{tip} is often used for shear-sensitive enzymes, microorganisms or other particles since high shear at the impeller tips can damage and inactivate microorganisms. The arising optimization problem of high dispersion efficiency versus particle strain has to be solved in numerous applications and the impact of stressful conditions on microorganisms or enzymes has been discussed by various authors (e.g., [28, 48]). Since size and shape, e.g., of mycelial pellets, often are a function of cultivation time, the process conditions might need to be constantly adjusted. In literature, various approaches to achieve a better understanding of these effects can be found, e.g., [25].

Concluding the discussion of the different impeller geometries and combinations (Sect. 2) with respect to scale-up, especially in biological applications on industrial scale, multiple impellers and tanks with high H/D ratio are commonly used since they provide a more homogeneous distribution of energy dissipation and are less harmful in terms of particle stress. They also offer other advantages such as high gas holdup, low power draw and high recirculation flows [48]. Multistage impellers lead to numerous new options such as the choice of stirrer number, type and spacing. Often different stirrer types such as radial and axial or mixed impellers are combined to achieve the best process conditions. While a combination of a certain number of 6-SBDTs seems to be the default option, with different combinations of axial and radial flow impellers, the description

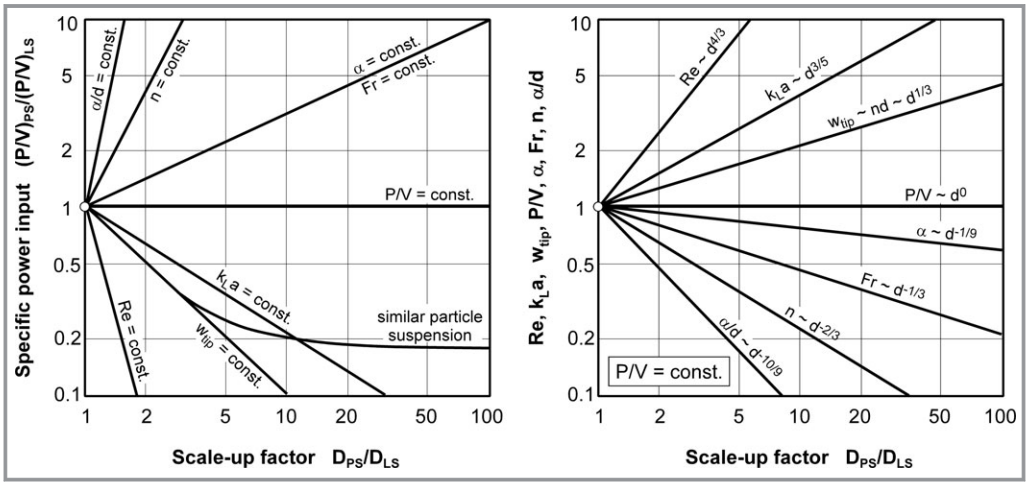

Figure 2. Effect of different scale-up criteria on the specific power input (left) and of the scale-up factors on different scale-up criteria (right; production scale, PS, lab scale, LS, heat transfer coeffcient, α).

and prediction of these processes and the scale-up becomes even more complex. The choice of stirrer types, number and spacing is crucial for the intended mixing process. Using CFD simulations, Letellier et al. [49] showed that problems arise with the common scale-up criterion P/V at geometrical similarity. This scale-up criterion should only be used if turbulent flow fields can be achieved for example by variation of geometrical parameters. Different fluid dynamics can induce flow compartmentation especially for a combination of radial flow impellers (see also [48]).

3.2 Scale-up Rules in Multiphase Systems

Various approaches towards a better fundamental understanding for scale-up rules, especially in multiphase systems, will be discussed in the following section.

3.2.1 Choice of Parameters and/or Plots to Characterize the Particle Size

The particle size distributions are crucial for multiphase processes since they eventually determine the final product quality but also the performance of the process itself. Measuring the particle size distributions and finding proper statistical parameters to characterize these distributions can be a complicated task. Particle sizes can be represented by different quantities varying from single parameters such as minimum (d_{min}), maximum (d_{max}), arithmetic (d_{10}) or Sauter mean diameter (d_{32}), distribution shape and width or the whole particle size distributions. The advantage of detailed distribution analysis lies in the higher information content and it is especially important if the distribution shape varies significantly between process conditions. Otherwise, important information might be lost leading to misinterpretation of results. For instance, Bliatsiou et al., Zhou et al. and Wille et al. [10, 50, 51] reported that the arithmetic mean droplet diameter or/and the median number-based diameter (d_{50}) failed to describe the breakage process in their stirred tank experiments. Single quantities as the Sauter mean diameter can represent numerous different distribution types [50]. Nevertheless, since a comparison of numerous complete distributions is not always easy to depict in clear graphs, the single quantities are often preferred to correlate particle size which, as mentioned before, can be misleading.

Fig. 3 depicts experimental drop size distributions in a stirred tank with rising agitation speed in various graph types. The impact of stirrer speed on Sauter mean diameter (Fig. 3a) is clearly visible. However, the Sauter mean diameter itself does not provide information on the distribution characteristics, as shown in Fig. 3b. The normalized distribution (Fig. 3c) does not allow drawing conclusions of the impact of agitation speed on the drop size, but on its effect on the distribution shape. Another option is a boxplot diagram that provides information on both drop size and distribution width and shape (Fig. 3d) and allows a better comparison between distributions in contrast to plotting numerous cases into one cumulative distribution diagram. A combination of several quantities such as characteristic diameter and information on distribution width and shape is always advantageous.

The particle size distributions can be additionally described or approximated by parameterized distribution functions with integral parameters [52, 53]. Such functional approximations are the Gates-Gaudin-Schuhmann distribution (GGS; simple approximation function of volume-based distributions), the Rosin-Rammler-Sperling-Bennet distribution (RRDB), the linear normal distribution (useful for coalescing systems), the logarithmic normal distribution (useful for not-coalescing systems) and the generalized extreme value distribution (GEV). Even though the use of such approximations is not often reported in literature, it can be advantageous especially when it comes to the complexities of scale-up or comparison of different process modes (batch vs. continuous process) or apparatuses (shaking flask vs. stirred tank).

Additional challenges are present when it comes to systems with non-uniform particle shapes, as apparent in numerous biological systems, crystallization processes or in systems where droplets or bubbles are elongated in the flow field. In such cases, other morphological particle characteristics have to be taken into consideration. For instance, Wucherpfennig et al. [54] introduced a morphology index to describe the morphology of filamentous fungi. The size and shape of these microorganisms vary between spherical pellets and filamentous mycelia depending on culture conditions. To obtain a correlation between morphology and size, the morphology number *MN* was defined incorporating the projected area, image analysis solidity, maximum diameter and elongation. To account for biological activity of the particle, Tang et al. [32] even defined the active part percentage (*APP*) of the pellet and compared it for different stirring conditions.

3.2.2 Correlations to Describe the Impact of Process Parameters on Particle Size

Correlations for particle sizes often describe the impact of process parameters on a chosen characteristic diameter of the system. Even if complex approaches such as population balance equations are used, results often are presented using only one chosen charateristic diameter. Independent of the type of result presentation the parameters determining the particle size distribution need to be understood in detail to identify correct correlations. Especially in breakage-dominated liquid-liquid systems, Weber number (*We*) correlations have been widely applied to predict Sauter mean or maximum diameters (e.g., [55]). Classical correlations describe the dependency of particle size on time *t*, specific power input P/V or tip speed w_{tip} (Tab. 3). However, several studies showed that these process parameters do not always suffice to correlate behavior (e.g., size, growth rate) of shear-sensitive microorganisms or drop sizes and to fully describe the breakage/dispersion mechanisms.

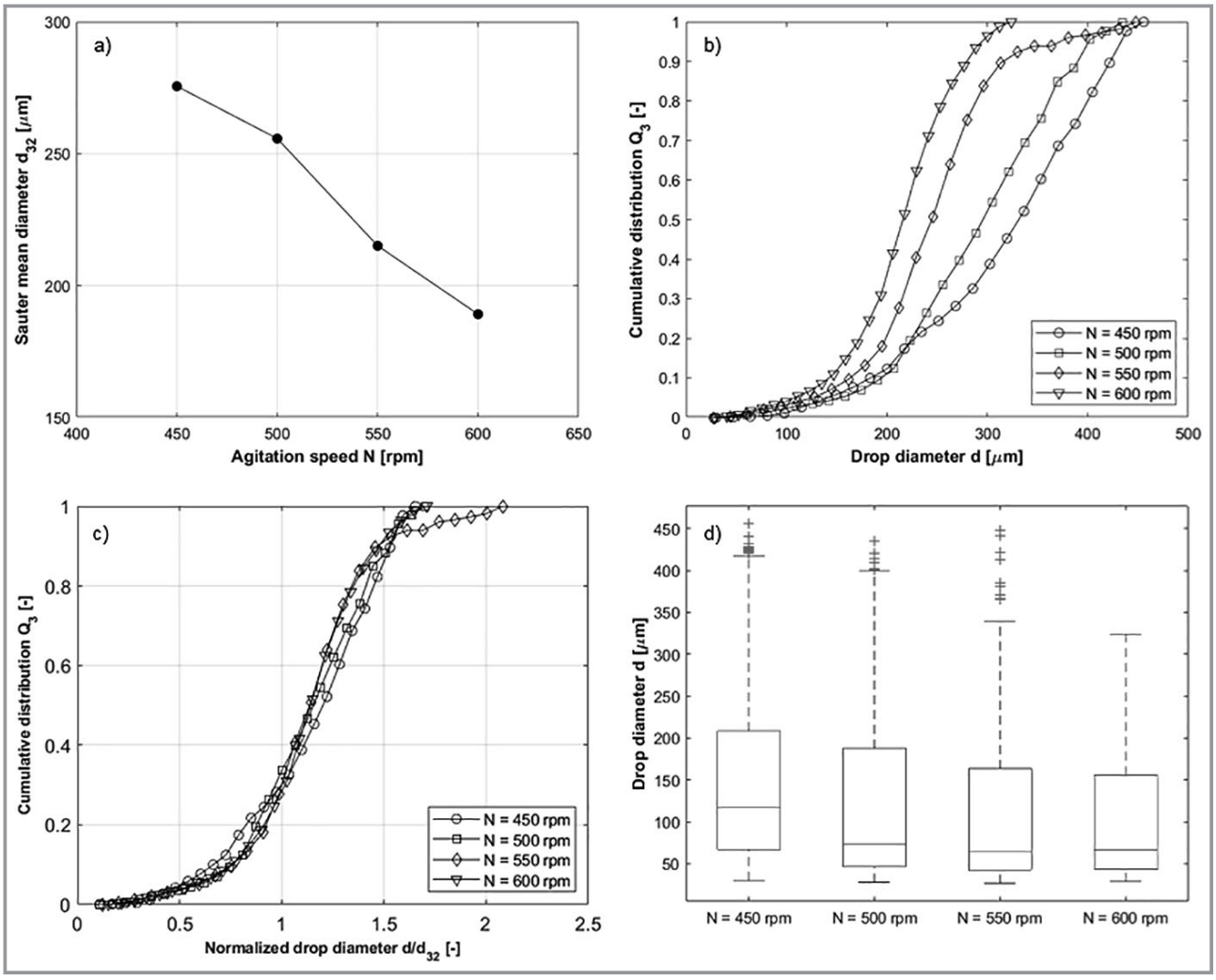

Figure 3. Examples for particle size presentation of the same cases (liquid-liquid system), a) Sauter mean diameter, b) cumulative particle size distribution, c) self-similarity presentation with cumulative particle size distribution divided by Sauter mean diameter, d) boxplot diagram of the particle size distributions.

The energy dissipation rate is often used as either a mean value for the overall tank $\bar{\varepsilon}$ or as local maximum values ε_{max} representing the highest strain particles have to endure in the tank. It is considered that the maximum energy dissipation is the fluiddynamic property mostly affecting particle strain, breakage or the disadvantageous stress of shear sensitive particles and microorganisms. The value of ε_{max} is not easy to be determined experimentally even with laser-based techniques and rather accessible with numerical approaches. Several authors related the maximum and mean energy dissipation rates $\varepsilon_{max}/\bar{\varepsilon}$ to describe particle breakage.

In literature, various ratios of $\varepsilon_{max}/\bar{\varepsilon}$ are reported even for intensively investigated stirrers (e.g., 6-SBDT), depending on the measurement technique and on the experimental or numerical approach. Gabriele et al. [62] summarized literature data for the $\varepsilon_{max}/\bar{\varepsilon}$ ratios of pitched blade impellers, showing that there is a huge variation in the results of different authors even for the same geometry (tank, impeller). Wollny [60] reviewed data for the $\varepsilon_{max}/\bar{\varepsilon}$ ratios of 6-SBDTs (Rushton turbines) with varying d/D ratios and pitched blade turbines. It was concluded, again, that the reported values in literature showed significant disagreement depending on the method and the applied approach (laser doppler anemometry LDA, PIV, CFD). The contradictory findings lead to misinterpretations when it comes to the characterization of various stirrer geometries as "high shear" or "low shear" impellers [10, 15, 60]. Thus, while in the past the axial flow impellers were considered as "low shear" agitators due to their lower power numbers and lower $\varepsilon_{max}/\bar{\varepsilon}$ values in comparison to the radial flow impellers (mainly Rushton turbine), multiple studies in particulate systems proved that particles stress produced by these stirrers is actually higher. Grenville et al. [61] pointed out that this incorrect characterization of the Rushton turbines was based on time-averaged velocity gradients. By determining the maximum kinetic energy dissipation rate within the

Table 3. Quantities correlated with particle sizes in stirred tanks with multiphase systems.

Size correlated with	Symbol	Exemplary references
Weber number	We	[55, 56]
time	t	[20, 21]
tip speed	w_{tip}	[50, 57]
specific energy input (whole tank volume)	P/V	[58]
specific energy input in impeller region	$P/(\rho V_I)$	[59]
mean energy dissipation rate	$\bar{\varepsilon} = \frac{P}{\rho V} = \frac{P}{M}$	[60]
normalized maximum energy dissipation rate	$\varepsilon_{max}/\bar{\varepsilon}$	[61]
energy dissipation and stirrer characteristic	$\frac{\bar{\varepsilon}}{F} = \frac{1}{F}\frac{P}{\rho V}$	[15]
energy dissipation circulation function	$EDCF = \frac{P}{V_I}\frac{1}{t_c}$	see Tab. 4
maximum energy dissipation circulation function	$EDCF_{max} = \varepsilon_{max}/t_c$	see Tab. 4

trailing vortex, they claimed that the Rushton turbines produce indeed lower dissipation (or stress) in comparison to hydrofoil impellers. Nevertheless, since measurements of the trailing vortices can be rather complicated and time-intensive, in present days, CFD seems to be the best way to determine these maxima reliably. At the same time, even though $\varepsilon_{max}/\bar{\varepsilon}$ is a crucial fluiddynamic property for the particle stress produced by an agitator, it is not the only key parameter to characterize the complex fluid dynamic phenomenon of particle breakage.

3.2.3 Specific Characterizations of Impeller Geometries

The determination of the impeller swept volume V_I where the highest energy dissipation rates occur is an important aspect in impeller characterization. Calculation of V_I is not trivial, especially when it comes to complex stirrer geometries as discussed in prior sections. PIV measurements of in- and out-pumping volume flow often do not balance regarding the flow around the impeller because of experimental uncertainties and lack of optical accessibility on the impeller blade tips. The impeller swept volume often corresponds to less than 1 % of the whole tank volume but certainly also depends on stirrer geometry [10, 60]. In the past, McManamey [63] approximated the impeller swept volume as a cylinder around the agitator with height and diameter according to the dimensions of the impeller. Henzler and Biederman [15] defined a geometrical characterization factor F for different impellers as an alternative to calculate the impeller swept volume V_I with

$$\frac{\varepsilon_{max}}{\bar{\varepsilon}} = \frac{c}{F} \tag{1}$$

where c is a constant (with c depending on the impeller type). The factor F can be calculated for different stirrer types and is defined as

$$F = \frac{P}{P_I}\frac{V_I}{V} = \left(\frac{d}{D}\right)^2\left(\frac{h}{d}\right)^{2/3} z^{0.6}(\sin\alpha)^{1.15} z_R^{2/3} \tag{2}$$

using the power input close to the impeller P_I or the blade angle α, blade height h, number of blades z and number of stirrers z_R. This equation was developed for standard stirrer types (6-SBDT, PROP, Mig and Intermig impeller, MIG, IMIG, blade and anchor stirrers, cross-arm stirrer). However, it cannot be applied for every impeller geometry. Nowadays, CFD seems more frequently being used to determine the impeller swept volume V_I, but so far, no uniform, broadly accepted critical value of shear stress to determine where the border between the different compartment lies is defined (see also [60]).

Another option for impeller characterization is the flow discharge number Fl that defines the pumping capacity in a given geometry

$$Fl = \frac{Q}{Nd^3} \tag{3}$$

using the flow rate Q (also called discharge flow). It is worth mentioning that also a circulation flow number Fl_c with the entrained flow Q_c can be calculated (with $Q_c \leq 2.5Q$ and $Fl_c = CD/d$ where C is a constant depending on impeller type and geometry) [64]. The direction of the primary flow depends on the stirrer geometry, which is obvious for classical axial or radial flow impellers but still needs to be determined for more complex impeller geometries. Numerous relations of power number N_P and discharge flow number Fl have been used to describe pumping efficiency, as summarized for example by Nienow [64]. The flow number for different impellers can be calculated based on the power number and geometrical parameter [16, 64, 65]. The circulation flow number, as an additional quantity, does not only consider the primary flow, but also the entrainment and recirculation. Hence, this value should also be considered for impeller characterization.

3.2.4 Developed Quantities in the Characterization of the Stirring Setups at Different Scales

As mentioned before, the terms "high shear" and "low shear" impellers are often insufficient to describe particle strain and microorganism behavior. One reason for this can be different circulation frequencies and residence times in the regions with high energy dissipation rates in impeller vicinity. In a study concerning the filamentous mold of *Peni-*

cillium chryosgenum, van Suijdam and Metz [66] introduced the concept of a dispersion zone where the breakage of hyphae takes place due to shear forces greater than the critical forces needed to break the filamentous structure. In this concept, the dispersion zone was determined not only by the shear stress (τ), but also by the size of the particles (L_e), since the critical shear stress (τ_{Le}) for breakage depends strongly on the particle specifications. The breakage frequency was then proportional to the frequency with which the particles pass through the dispersion zone V_{disp}. Based on some assumptions, the volume of this zone V_{disp} was proportional to

$$V_{disp} \sim N^{0.75} D^{3.5} / \varepsilon_{loc}^{0.25} \tag{4}$$

(ε_{loc} being the local energy dissipation rate) and, furthermore, the breakup frequency f was proportional to

$$f \sim N^{1.75} D^{0.5} L_e / d^{0.38} \tag{5}$$

Reuß [67] tried to describe the mechanical damage of *Rhizopus nigricans* in stirred bioreactors. The suggested concept was based on an analogy to a mechanical disintegration process earlier approached by Weit and Schwedes [68]. In this concept the power input per circulated flow rate

$$P/Q = \frac{P}{V/t_c} \tag{6}$$

with t_c as the circulation time was used as key parameter to correlate the experimental data of mechanical damage of the microorganisms. The recirculation time distributions in the stirred tank were measured using the magneto flow follower technique. For 100-L and 3000-L vessels the mean circulation time could be correlated with Eq. (7)

$$Nt_c = 0.76 \left(\frac{H}{D}\right)^{0.6} \left(\frac{D}{d}\right)^{2.7} \tag{7}$$

Both the experimental data for *R. nigricans* as well as older published data for the disruption of the protozoa *Tetrahymena pyriformis* could be correlated with $\frac{P}{V/t_c}$. The circulation time is sometimes also expressed as a function of mixing time θ using [69]

$$4t_c = \theta \tag{8}$$

In the work of Smith et al. [70], a correlation was established between the agitation and the morphology and productivity of *Penicillium chrysogenum* at 10-L and 100-L scale. The aforementioned suggested approach from Reuß [67] gave a poor correlation of the results for *P. chrysogenum* at these scales. At the same time, the circulation times obtained using Reuß's approximation differentiated strongly from those calculated using the pumping capacity of the agitators

$$\frac{1}{t_c} = Fl\, N \frac{D^3}{V} \tag{9}$$

It is worth mentioning here that this could be calculated with the circulation flow number Fl_c, as well, even though this has not been discussed in literature yet. Therefore, Smith et al. [70] based their work on the concept of dispersion regions by van Suijdam and Metz [66]. In this way, the breakage in the stirred tank was considered the result of the exposure to a regime of high energy dissipation at a frequency related to the circulation time. Modifying the expression of van Suijdam and Metz [66] for the power input, the final proposed model by Smith et al. [70] was

$$f \sim P/\left(D^3 t_c\right) \tag{10}$$

With this model, the recorded data of the penicillin production showed good qualitative agreement for both scales (10 L and 100 L).

Shortly after the study of Smith et al. [70], Makagiansar et al. [71] used the same strain and proved additionally the suitability of $P/(D^3 t_c)$ as correlating parameter for the morphology and the productivity of *P. chrysogenum* at scales of 5 L, 100 L and 1000 L.

Both studies of Smith et al. and Makagiansar et al. [70, 71] were conducted with only one impeller type (6-SBDT). However, the work of Biedermann and Henzler [58] showed the influence of impeller type and geometry on various particulate systems. Motivated by those findings, Jüsten et al. [16] investigated the dependence of *P. chrysogenum* morphology on the impeller geometry. In that study, 12 impeller types were tested. The model of Smith et al. [70] was modified by a geometrical factor k defined as

$$k = \frac{\pi}{4} \frac{W}{d} \tag{11}$$

with W as the projected blade height. With this factor, the impeller swept volume for each impeller geometry was calculated individually ($V_I = kD^3$) and the correlating function was transformed to

$$EDCF = \frac{P}{V_I t_c} = P/\left(kD^3 t_c\right) \tag{12}$$

The newly introduced mixing parameter was called energy dissipation circulation function (*EDCF*). Jüsten et al. [16] underlined the difficulty to measure the energy dissipation rates near the impeller and suggested a further approximation considering the presence of trailing vortices in the impeller swept volume. Therefore, they additionally modified the factor k to the factor

$$k' = N_V k \tag{13}$$

where N_V is the number of trailing vortices for the impeller under investigation divided by the number of trailing vorti-

ces for a 6-SBDT. Including vortices, *EDCF* was expressed as $P/(k' D^3 t_c)$. Both expressions of *EDCF*, i.a., $(P/(kD^3 t_c)$ and $P/(k' D^3 t_c))$ correlated at a great degree with the experimental data of *P. crysogenum* at 1.4-L, 20-L and 180-L scale of unaerated tanks and were, therefore, suggested as scale-up criterion. In a follow-up study, Jüsten et al. [72] additionally proved the suitability of *EDCF* to depict the impeller influence not only on the morphology but also on the growth and productivity of *P. chrysogenum* in a 6-L fed-batch fermentation process.

Applying the *EDCF* concept and the approximation for $P/(kD^3)$ and t_c as suggested by Jüsten et al. [16], various studies correlated effectively data of *P. chrysogenum, Aspergillus oryzae, Aspergillus terreus* and *Trichoderma harzianum* cultivations (see Tab. 4).

In more recent works, an effort was made to determine more precisely both the maximum energy dissipation rate ε_{max} and the circulation frequency $1/t_c$. Xia et al. [23] applied in their study the *EDCF* for the cultivation of *Streptomyces avermitilis*. However, they calculated both terms of the function ($P/(kD^3)$ and t_c) numerically by means of CFD. Comparing the *EDCF* function in their work with that of Jüsten et al. [16], a significant deviation was reported, which was mainly attributed to the different calculation methods. Similarly, Hardy et al. [28] used the *EDCF* as scale-up criterion for *Trichoderma reesei* fermentation. They estimated the maximum local energy dissipation rate ε_{max} according to Grenville et al. [61] instead of using Jüsten's approximation $P/(kD^3)$ while the circulation time was still calculated with the pumping rate of the impeller. This leads to the function

$$EDCF_{max} = \frac{\varepsilon_{max}}{t_c} \tag{14}$$

They showed that this approach can correlate observed effects such as that "low shear" impellers pose a high particle stress on microorganisms due to high frequencies with which the particles pass through the impeller swept volume.

Finally, the last evolution of Jüsten's *EDCF* mixing parameter was recently reported in the work of Liu et al. [73] for the cultivation of *Carthamus tinctorius L.* cells. Euler-Langrage model based CFD was employed to calculate accurately the maximum shear stress and the frequency of particle circulation through the high-shear regime in the stirred bioreactor. The product of maximum shear stress and shear frequency of particle (*SSF*) was defined and successfully applied to establish a relationship between the cell death rate and the shear environment.

The concept of *EDCF* or *SSF*, even though it has been mainly applied so far in biotechnological stirring processes, is potentially relevant for other multiphase systems, as well. For instance, Zhou and Kresta [50] worked with a liquid-liquid coalescing system. In an effort to correlate the measured Sauter mean drop diameter with a process parameter they concluded that when the mean energy dissipation rate was implemented, no grouping of the data was achieved with the measured d_{32} being widely scattered. When the

Table 4. Studies applying the EDCF concept.

Reference	Biological system	Varied parameters	Reactor liquid volume V	Correlated property	Remark
[16, 72]	*Penicillium chrysogenum*	impeller geometry, rotational speed, scale	1.4 L, 6 L, 20 L, 180 L	morphology, productivity	
[74]	*Aspergillus oryzae, Penicillium chrysogenum*	impeller geometry, rotational speed	1.4 L	morphology	offline fragmentation experiments
[75]	*Aspergillus oryzae*	rotational speed	80 m^3	k_La, productivity	
[76]	*Aspergillus terreus*	rotational speed	5 L	k_La, morphology, productivity	
[65, 77]	*Trichoderma harzianum*	rotational speed	10 L	morphology, growth, productivity	additional independent study of effect of the *EDCF* components $P/(kD^3)$ and t_c over mycelial fragmentation
[23]	*Streptomyces avermitilis*	impeller geometry and combination	35 L	morphology	energy dissipation rates and circulation time distributions numerically calculated
[32]	*Aspergillus niger*	impeller geometry	35 L	morphology	active pellet part (*APP*) definition
[73]	*Carthamus tinctorius* L. cells	rotational speed, scale	5 L, 15 L	cell death rate	shear stress and circulation frequency numerically calculated
[28]	*Trichoderma reesei*	impeller diameter, rotational speed	2.5 L, 80–130 m^3	morphology, growth, rheology	differentiation in calculation of ε_{max} and t_c

mean flow velocity, expressed as tip speed derivative Nd, was used to correlate the drop breakup, a differentiation between the 6-SBDT and the axial flow impellers appeared. When d_{32} was related to ε_{max}, the impellers were grouped into high power number and low power number stirrers. Finally, the best grouping of the data was achieved when the regression of d_{32} vs. $\varepsilon_{max}Nd^2$ was implemented, where Nd^2 correlated with the circulation frequency $1/t_c$, making this a variation of the *EDCF* approach (as only one liquid-liquid dispersion was tested, Nd^2 worked although usually the Reynolds number $Re = Nd^2/\nu$ might be used).

The definition of an impeller swept volume and a bulk volume with comparatively low shear rates also is the basic idea for compartment modeling approaches. These can be performed with different numerical tools ranging from population balances to complex CFD simulations. More information on the detailed turbulence in the impeller vicinity is of great importance for these approaches. The turbulence and energy dissipation near the stirrer blade is a field of study where significant efforts are made to improve the fundamental understanding. Lee and Yianneskis [78] determined the time and length scales of turbulence in a stirred tank with a 6-SBDT using two component LDA in back scatter mode to estimate dissipation rates of turbulence energy. They found that the flow is mostly anisotropic near the blades. Grenville et al. [61] summarised power numbers, flow numbers and trailing vortice length for different stirrers. The trailing vortex kinetic energy can be scaled by tip speed squared [61]. The vortex length scale l_v can be determined as an additional characteristic of impellers. The character of trailing vortices can also be analyzed using sophisticated numerical methods such as Lattice Boltzmann large eddy simulaitons. Information can be used in addition, e.g., to circulation frequency to quantify the characteristics of different stirrer types.

3.2.5 Modeling and Simulation of Complex Flow Fields Using Different Levels of Detail

CFD is a useful tool to characterize single and multiphase systems. Turbulence models are constantly refined and the incorporation of population balances into CFD simulations to describe multiphase systems is a task addressed by many researchers. CFD can provide information, e.g., on local shear, temperature, energy dissipation or momentum. State of the art are Eulerian multiphase approaches considering phase interactions by various correlation-based closures (e.g., for drag and lift force or mass/heat transfer and turbulence models). The mesh size is a critical issue especially considering the description of processes on various scales or for the determination of local energy dissipation. Other methods might be necessary to describe the behavior of particle swarms, such as molecular dynamics or Lattice Boltzmann methods [79]. For stirred tanks, fully turbulent simulations where spatial inhomogeneity does not have to be considered clearly dominate.

A complete and reliable description of flow and turbulence even in simple, single-phase stirred tanks is, however, not obtained yet. Reasons are the broad time and length scales that occur in turbulent flow regimes. According to the energy cascade theory, the length scales range from the turbine blade size down to the Kolmogorov length. Hence, it is nearly impossible to obtain a fully resolved picture of the turbulent flow field. Gillissen and van den Akker [80] compared direct numerical simulations (DNS) to large eddy simulations (LES) and Reynolds-averaged Navier-Stokes simulations (RANS). The data for validation can (to some degree) be obtained by PIV and LDA measurements. Conventional CFD approaches do not aim to resolve the complete flow field but model the effect of turbulence eddies on the average flow field. RANS simulations solve the mean flow and adopt a model to incorporate turbulent fluctuations. This leads to the fact that turbulence levels are often underpredicted by RANS. Especially when the time scales of chemical or physical operations are similar or smaller than the turbulent time scales, processes can depend severely on details of turbulence [80]. LES simulations intend to explicitly not calculate the complete turbulent energy spectrum. In comparison to RANS, where the complete spectrum of turbulence is modeled, LES only models the effect of higher frequencies of the spectrum (of eddies smaller than the grid spacing) using subgrid-scale models. Hence, it provides more details and is more suitable when specific turbulence characteristics are important. Problems arise in LES when interactions with solid walls are relevant, because some underlying assumptions break down due to the anisotropic and non-equilibrium nature of these regions. Both RANS and LES approaches imply a loss of information so that they are still an approximation to reality. The anisotropic nature of, e.g., vortices has been shown by Lee and Yianneskis [78], as mentioned before. Since the vortex region is where high energy dissipation occurs, it is relevant for breakage and particle stresses. Hence, being able to explicitly calculate the turbulence would be beneficial. However, there always is the trade-off between grade of detail and calculation time or computing power capacity. DNS could be used to fully resolve all length scales in the turbulent flow field without any modeling. If all eddies are fully resolved, DNS has the potential to replace experiments, provide reference data for RANS and LES submodels and further develop CFD into a measurement tool. Gillissen and van den Akker [80] performed DNS simulations in a standard stirred tank geometry with baffles using 2.9×10^9 grid points but still pointed out that this number might not be sufficient to resolve the Kolmogorov length in the wake of the turbine blades and the smallest eddies of the system.

In lab scale, the assumption of homogeneity often holds true, but this is frequently not the case in large-scale applications where a drastic decline in process performance can occur due to inhomogeneity. Especially in large-scale or fed-batch bioreactors, imperfect mixing can lead to concentration gradients with a lack or excess of oxygen or other substrates. Fluid dynamic inhomogeneities in large-scale

stirred tanks can lead to unpredicted effects as recently reported by Rosseburg et al. [81]. Hence, mixing models and biokinetics need to be combined to adequately predict process performance [82].

Microorganisms in agitated tanks follow certain pathways and experience different environmental conditions. These conditions vary not only in terms of shear as discussed before in the *EDCF* approach, but also in local concentrations of oxygen, substrates or waste products. The response of the cells to these dynamic conditions is not fully understood yet. It still has to be clarified which substances influence the reaction and response of cells, which effect repeated exposure to unfavorable microenvironmental conditions (concentrations, particle stress) has and how often and how long this exposure does occur. A better understanding on how their history affects the microorganism performance and changes the response of microorganisms to stress conditions is crucial. Similar to the *EDCF* approach, current studies try to combine fluid dynamics with dynamic biological models and biokinectics. To assess bioreactor performance, a reliable model for scale-up based on the concept of microbial environment is crucial. The performance of an industrial bioreactor, hence, is determined by two types of factors: factors that define the capacity of cells (concentrations of nutrients) and factors that control the physical environment such as flow properties [82]. The physical environment of a reactor should be mapped, and the biological response needs to be computed as detailed as possible. Therefore, the question arises how detailed the model needs to be.

Both hydrodynamic and biological parameters are not easy to quantify. Single unfavorable parameters are investigated using scale-down approaches such as in unstirred bypass loops to clarify the effects of, e.g., oxygen limitations, excess sugars, pH or similar conditions ([46], see also [82, 83]). The governing stress conditions can be tracked and quantified, but the sort and number of parameters that can be determined is limited. Simulation of cell growth can be performed using hyperbolic Monod kinetics. However, this model to describe cell growth often fails on large scale. Therefore, various sophisticated models to describe inhibition effects are investigated in literature while also focusing on the modeling of intracellular biochemical reactions and simulations of rapid changes in microorganism environment.

To model the fluid dynamic mixing process in stirred (often aerated) tanks, different approaches can be used. Most of them divide the reactor into basic units, but this can be performed using different length scales. Compartment models can be applied where the tank is divided into ideally mixed zones and plug flow zones (cascade of ideal tanks). The microorganisms traveling through different regions can be described using a history function F_{history} as proposed by Guillard and Trägårdh [82]. F_{history} is not a constant but varies over time and corresponds to a hyperbolic model with competitive inhibition. Gas flow can be implemented by superimposing the flow pattern induced by bubbles on the fluid flow. Mass exchange can be calculated according to volume considerations and Froude number *Fr*. The reactor can also be divided into ideally mixed volumes or cells where each cell is connected to neighbors by convective flows related to the pumping capacity of the impeller and diffusional flows. These approaches were also improved by considering reaction, gas flow or multiple impellers.

4 Conclusion

The aim of this article was reviewing single and multistage impeller systems and possibilities to quantify such systems in terms of performance and scale-up with respect to aerated stirred tanks used in the cultivation of biological products. Nienow [3] collected a guideline on how to choose the right setup for cell cultivation based on seven points. While four of them are rather related to the operation, the other three are rather related to the design of the setup. A liquid height to tank diameter $H/D > 1$ should be chosen to reduce the overall impact of the shear due to bubble bursts at the surface. A high-power motor with variable speed should be used to keep the oxygen transfer rate above the oxygen uptake rate, even with changing rheology of the broth. Furthermore, a multistage setup of wide-blade up-pumping impellers is suggested to ensure a good bubble dispersion and homogeneous conditions within the tank. Most of these conditions were found in the reviewed studies but mostly not at the same time. Still, while generally the guideline by Nienow [3] can definitely be confirmed by recent studies as, e.g., it can be stated with almost absolute certainty that a multistage setup consisting only of 6-straight bladed disc impeller (Rushton turbine) should be avoided. The details of how to choose the impellers and impeller combination still remains challenging.

When it comes to microbial development, homogeneity within the system appears to be the crucial factor. This incorporates homogeneity of all components within the reactor but also (as far as possible) homogeneity regarding shear. These aims can contradict making the choice of the impellers in a multistage arrangement a difficult exercise. Commonly used parameters in the field of stirred tanks (with multiphase systems) fail at helping to understand the behavior and, furthermore, do not allow a scale-up from lab-scale to industrial size fermenters as these are too global. Intermediate steps taking local impeller-specific information into account lead towards compartment approaches. This can be either done by backmixing or dispersion approaches describing virtually the behavior by combining ideal reactors (ideal stirred tank and ideal plug flow) with certain volume exchanges between each other. Leading into the same direction the approaches taking system-specific information such as swept volume, circulation time or maximum energy dissipation into account seem more applicable. Still, for a proper calculation of these quantities,

especially for new impeller designs and multistage configurations with communicating flow regions, CFD simulations are an unavoidable necessity but still include models for certain conditions. Finally, purely numerical approaches would be a possibility, as well, to understand and properly scale up the biological systems. Still, for these cases, extremely fine grids would be necessary to resolve turbulent fluctuations affecting the integrity and growth characteristic of the microorganisms. For the type of growth (e.g., for fungi as pellets or mycelial), the biomass development and the productivity and exact knowledge about quantitative data of the metabolism is necessary. Realistically, neither the biological information will be completely accessible for all cultivations of interest, nor will, in the near future, the computational power be obtainable at reasonable cost.

Therefore, the intermediate approach, e.g., using the energy dissipation circulation function or derivates of it, appears to be the most useful tool at the moment and proved already to be very useful in the field of cultivation. In some works, the best impeller combination with respect to biological performance had the lowest value for this function. Furthermore, it was used in generalized correlations describing numerous impeller types and can be used as a scale-up criterion for biological systems.

This work is part of the Collaborative Research Center/ Transregio 63 "Integrated Chemical Processes in Liquid Multiphase Systems" (DFG SFB/TR 63) and the Priority Programs “Dispersity-, structural, and phase- changes of proteins and biological agglomerated in biotechnological processes” (DFG SPP1934) and “Reactive Bubbly Flows” (DFG SPP1740). Financial support by the Deutsche Forschungsgemeinschaft is gratefully acknowledged. The authors would like to thank Fritzi Laura Stephan for providing the examples for experimental particle size distributions and Nico Jurtz for CFD consulting.

Lutz Böhm graduated in the field “Process and Energy Engineering” at Technische Universität Berlin in 2009 and, afterwards, started working at the Chair of Chemical and Process Engineering. In 2015, he successfully defended his PhD thesis “Comparison of single bubble and bubble swarm behavior in narrow gaps inside flat sheet membrane modules”. Since then, he works as a postdoctoral fellow in the field of “Transport phenomena in reactive Newtonian and non-Newtonian multiphase systems”.

Lena Hohl studied chemical engineering at the Technische Universität Dresden until 2014. Shortly afterwards, she started working at the Chair of Chemical and Process Engineering of the Technische Universität Berlin, defended her PhD thesis on dispersion and phase separation in complex liquid multiphase systems in 2018 and is a postdoctoral fellow in this field of study ever since.

Chrysoula Bliatsiou studied chemical engineering at National Technical University of Athens and environmental and process engineering at University of Stuttgart. Since 2016 she works at the Chair of Chemical and Process Engineering at Technische Universität Berlin in the field of multiphase stirring processes with special focus on biotechnological applications.

Matthias Kraume studied chemical engineering at the University of Dortmund and received his PhD with a thesis on direct contact heat transfer. He then worked for nine years, first as a development engineer and later as a project engineer for BASF, Ludwigshafen. Since 1994 he is Professor of Chemical Engineering at the Technical University Berlin. His research fields are transport phenomena in multiphase systems, membrane processes, and stirred tanks.

Symbols used

c	[–]	constant
C	[–]	constant
d	[m]	impeller diameter
d_{10}	[m]	arithmetic mean diameter of the particle
d_{32}	[m]	Sauter mean diameter of the particle
d_{50}	[m]	median diameter of the particle
d_{min}	[m]	smallest diameter of the particle
d_{max}	[m]	largest mean diameter of the particle
D	[m]	vessel diameter
D_{LS}	[m]	diameter of vessel in lab scale
D_{PS}	[m]	diameter of vessel in lab scale
$EDCF$	[W m^{3}s^{-1}]	energy dissipation circulation function
$EDCF_{max}$	[W m^{3}s^{-1}]	maximum energy dissipation circulation function
f	[s^{-1}]	breakup frequency
F	[–]	geometrical characterization factor
$F_{history}$	[–]	time variable history function
Fl	[–]	flow discharge number
Fl_c	[–]	circulation flow number
Fr	[–]	Froude number
H	[m]	filling height of the liquid in the tank
J	[–]	number of impellers in a multistage configuration
k	[–]	geometrical factor
k'	[–]	modified geometrical factor
K	[Pa s^m]	consistency index
k_La	[s^{-1}]	volumetric oxygen transfer rate
l_v	[m]	vortex length scale
L_e	[m]	size of the particles
m	[–]	flow index
M	[kg]	mass
MN	[–]	morphology number
n	[–]	exponent
N	[s^{-1}]	rotational speed
N_P	[–]	power number
$N_{P,1}$	[–]	power number of a single 6-SBDT
$N_{P,total}$	[–]	power number of a multistage configuration
N_V	[–]	number of trailing vortices divided by the number of trailing vortices of an 6-SBDT
Ne	[–]	Newton number, equal to N_P
P	[W]	power input
P_l	[W]	power input close to the impeller
Q	[m^{3}s^{-1}]	discharge liquid flow rate
Q_c	[m^{3}s^{-1}]	entrained liquid flow rate
Q_g	[m^{3}s^{-1}]	gas flow rate
Re	[–]	Reynolds number
SSF	[Pa s^{-1}]	product of maximum shear stress and shear frequency of particles
t_{95}	[s]	mixing time for 95 % homogeneity
t_c	[s]	circulation time
V	[m^3]	reactor liquid volume
V_{disp}	[m^3]	dispersion zone near the impeller
V_l	[m^3]	impeller swept volume
w_{tip}	[m s^{-1}]	tip speed of the impeller
W	[m]	projected blade height
We	[–]	Weber number
z	[–]	number of blades
z_R	[–]	number of impellers

Greek letters

α	[rad]	blade angle
α	[Wm^{2}K]	heat transfer coefficient
$\dot{\gamma}$	[s^{-1}]	shear rate
$\bar{\varepsilon}$	[W kg^{-1}]	mean energy dissipation
ε_{loc}	[W kg^{-1}]	local energy dissipation
ε_{max}	[W kg^{-1}]	maximum energy dissipation
θ	[s]	mixing time
μ	[Pa s]	dynamic viscosity
ν	[m^{2}s]	kinematic viscosity
ρ	[kg m^3]	density
τ	[Pa]	shear stress
τ_{Le}	[Pa]	critical shear stress for particle breakage

Abbreviations

2-SB	2-straight blade impeller
3-HYDRO	3-blade hydrofoil impeller
3-HYDRO-U	up-pumping 3-blade hydrofoil impeller
3SHPU	up-pumping 3-bladed Scaba axial hydrofoil impellers
3-PB	3-pitched blade turbine
4-HYDRO-U	up-pumping 4-blade hydrofoil impeller
4-PB	4-pitched blade turbine
6-ABDT	6-arrowy blade disc turbine
6-CB	6-curved blade impeller
6-CBDT	6-curved blade disc turbine
6-PB	6-pitched blade turbine
6-PBflex	6-pitched flexible blade turbine
6-PBflexP	6-pitched punctured flexible blade turbine
6-PBU	up-pumping 6-pitched blade turbine
6-SBDT	6-straight blade disc turbine (also called Rushton turbine)
6-SBDT-6-PB-flex	top-bottom) 6-SBDT and 6-PB connected (with flexible bands
6-SBDT-6-PB-flexP	top-bottom) 6-SBDT and 6-PB connected (with flexible punctured bands
6-SBDT-6-	two 6-SBDTs connected with flexible bands

SBDT-flex	
6-SBDTflex	6-straight flexible blade disc turbine
6-SBflex	6-straight flexible blade impeller
A310	Lightnin A310
A315	Lightnin A315
B2-45	Hayward Tyler B2-45
BiLOOP	up-pumping bionic-loop impeller
BT-6	Chemineer BT-6
CD-6	hollow-type six-bladed concave disc turbine
CEPET	centripetal turbine
CFD	computational fluid dynamics
CPU	central processing unit
DHR	double helical ribbon
DNS	direct numerical simulation
EED	down-pumping elephant ear impeller
EEU	up-pumping elephant ear impeller
EI	ellipse impeller
FE	finite element method
FZ	Fullzone® impeller
HDY675	6-radial Smith turbine half pipe blades
GEV	generalized extreme value distribution
GGS	Gates-Gaudin-Schuhmann distribution
GI	gate impeller
IMIG	Intermig impeller
LDA	laser doppler anemometry
LE20	Hayward Tyler LE20
LES	large eddy simulation
LLE	largest Lyapunov exponent
MB	Maxblend® impeller
MIG	Mig impeller
MFLOWT	Prochem Max Flow T
OTR	oxygen transfer rate
OUR	oxygen uptake rate
PBE	population balance equation
PIV	particle image velocimetry
PROP	down-pumping propeller
PROP-R	down-pumping propeller with ring
RANS	Reynolds-averaged Navier-Stokes simulation
RRDB	Rosin-Rammler-Sperlling-Bennet distribution
SS	Swingstir® impeller
TRIB	profiled triblade
WRIB	wave-ribbon impeller

References

[1] E. L. Paul, V. A. Atiemo-Obeng, S. M. Kresta, *Handbook of industrial mixing: science and practice*, John Wiley & Sons, New York **2003**.

[2] S. M. Kresta et al., *Advances in industrial mixing: a companion to the handbook of industrial mixing*, John Wiley & Sons, Hoboken, NJ **2015**.

[3] A. W. Nienow, *Cytotechnol.* **2006**, *50 (1)*, 9. DOI: https://doi.org/10.1007/s10616-006-9005-8

[4] V. G. Pangarkar, *Design of multiphase reactors*, John Wiley and Sons, Hoboken, NJ **2015**.

[5] Z. Li, Y. Bao, Z. Gao, *Chem. Eng. Sci.* **2011**, *66 (6)*, 1219–1231. DOI: https://doi.org/10.1016/j.ces.2010.12.024

[6] A. Ochieng, M. S. Onyango, A. Kumar, K. Kiriamiti, P. Musonge, *Chem. Eng. Process.* **2008**, *47 (5)*, 842–851. DOI: https://doi.org/10.1016/j.cep.2007.01.034

[7] A. W. Nienow, W. Bujalski, *Chem. Eng. Res. Des.* **2004**, *82 (9)*, 1073–1081. DOI: https://doi.org/10.1205/cerd.82.9.1073.44150

[8] H. Zhu, A. W. Nienow, W. Bujalski, M. J. H. Simmons, *Chem. Eng. Res. Des.* **2009**, *87 (3)*, 307–317. DOI: https://doi.org/10.1016/j.cherd.2008.08.013

[9] G. Montante, A. Paglianti, *Chem. Eng. J.* **2015**, *279*, 648–658. DOI: https://doi.org/10.1016/j.cej.2015.05.058

[10] C. Bliatsiou, A. Malik, L. Böhm, M. Kraume, *Ind. Eng. Chem. Res.* **2019**, *58 (7)*, 2537–2550. DOI: https://doi.org/10.1021/acs.iecr.8b03654

[11] N. Ghobadi, C. Ogino, T. Ogawa, N. Ohmura, *Bioprocess. Biosyst. Eng.* **2016**, *39 (11)*, 1793–1801. DOI: https://doi.org/10.1007/s00449-016-1653-2

[12] N. Ghobadi, C. Ogino, T. Ogawa, N. Ohmura, *J. Chem. Eng. Jpn.* **2018**, *51 (2)*, 143–151. DOI: https://doi.org/10.1252/jcej.17we010

[13] Y. Liang, D. Shi, B. Xu, Z. Cai, Z. Gao, *AIChE J.* **2018**, *64 (11)*, 4148–4161. DOI: https://doi.org/10.1002/aic.16353

[14] F. Qiu, Z. Liu, R. Liu, X. Quan, C. Tao, Y. Wang, *Exp. Therm Fluid Sci.* **2018**, *97*, 351–363. DOI: https://doi.org/10.1016/j.expthermflusci.2018.04.006

[15] H.-J. Henzler, A. Biedermann, *Chem. Ing. Tech.* **1996**, *68 (12)*, 1546–1561. DOI: https://doi.org/10.1002/cite.330681205

[16] P. Jüsten, G. C. Paul, A. W. Nienow, C. R. Thomas, *Biotechnol. Bioeng.* **1996**, *52 (6)*, 672–684. DOI: https://doi.org/10.1002/(SICI)1097-0290(19961220)52:6<672:AID-BIT5>3.0.CO;2-L

[17] Y. L. Young, *J. Fluids Struct.* **2008**, *24 (6)*, 799–818. DOI: https://doi.org/10.1016/j.jfluidstructs.2007.12.010

[18] R. L. Campbell, E. G. Paterson, *J. Fluids Struct.* **2011**, *27 (8)*, 1376–1391. DOI: https://doi.org/10.1016/j.jfluidstructs.2011.08.010

[19] M. Luhar, H. M. Nepf, *J. Fluids Struct.* **2016**, *61*, 20–41. DOI: https://doi.org/10.1016/j.jfluidstructs.2015.11.007

[20] S. Maaß, F. Metz, T. Rehm, M. Kraume, *Chem. Eng. J.* **2010**, *162 (2)*, 792–801. DOI: https://doi.org/10.1016/j.cej.2010.06.007

[21] S. Maaß, T. Rehm, M. Kraume, *Chem. Eng. J.* **2011**, *168 (2)*, 827–838. DOI: https://doi.org/10.1016/j.cej.2011.01.084

[22] F. Magelli, G. Montante, D. Pinelli, A. Paglianti, *Chem. Eng. Sci.* **2013**, *101*, 712–720. DOI: https://doi.org/10.1016/j.ces.2013.07.022

[23] J.-Y. Xia, Y.-H. Wang, S.-L. Zhang, N. Chen, P. Yin, Y.-P. Zhuang, J. Chu, *Biochem. Eng. J.* **2009**, *43 (3)*, 252–260. DOI: https://doi.org/10.1016/j.bej.2008.10.010

[24] M. Cai, X. Zhou, J. Lu, W. Fan, C. Niu, J. Zhou, X. Sun, L. Kang, Y. Zhang, *Bioresour. Technol.* **2011**, *102 (3)*, 3584–3586. DOI: https://doi.org/10.1016/j.biortech.2010.10.052

[25] Y. Yang, J. Xia, J. Li, J. Chu, L. Li, Y. Wang, Y. Zhuang, S. Zhang, *J. Biotechnol.* **2012**, *161 (3)*, 250–256. DOI: https://doi.org/10.1016/j.jbiotec.2012.07.007

[26] N. Suhaili, J. S. Tan, M.-S. Mohamed, M. Halim, A. B. Ariff, *Asia-Pac. J. Chem. Eng.* **2015**, *10 (1)*, 65–74. DOI: https://doi.org/10.1002/apj.1846

[27] X. Zhao, L. Ren, D. Guo, W. Wu, X. Ji, H. Huang, *Bioprocess. Biosyst. Eng.* **2016**, *39 (8)*, 1297–1304. DOI: https://doi.org/10.1007/s00449-016-1608-7

[28] N. Hardy, F. Augier, A. W. Nienow, C. Béal, F. B. Chaabane, *Chem. Eng. Sci.* **2017**, *172*, 158–168. DOI: https://doi.org/10.1016/j.ces.2017.06.034

[29] P. Vrábel, R. G. J. M. van der Lans, K. C. A. M. Luyben, L. Boon, A. W. Nienow, *Chem. Eng. Sci.* **2000**, *55 (23)*, 5881–5896. DOI: https://doi.org/10.1016/S0009-2509(00)00175-5

[30] M. C. C. Bustamante, M. O. Cerri, Alberto C. Badino, *Chem. Eng. Sci.* **2013**, *90*, 92–100. DOI: https://doi.org/10.1016/j.ces.2012.12.028

[31] M.-H. Xie, J.-Y. Xia, Z. Zhou, G.-Z. Zhou, J. Chu, Y.-P. Zhuang, S.-L. Zhang, H. Noorman, *Chem. Eng. Sci.* **2014**, *106*, 144–156. DOI: https://doi.org/10.1016/j.ces.2013.10.032

[32] W. Tang, A. Pan, H. Lu, J. Xia, Y. Zhuang, S. Zhang, J. Chu, H. Noorman, *Biochem. Eng. J* **2015**, *99*, 167–176. DOI: https://doi.org/10.1016/j.bej.2015.03.025

[33] M. M. Buffo, L. J. Corrêa, M. N. Esperança, A. J. G. Cruz, C. S. Farinas, A. C. Badino, *Biochem. Eng. J* **2016**, *114*, 130–139. DOI: https://doi.org/10.1016/j.bej.2016.07.003

[34] L. J. Correa, A. C. Badino, A. J. G. Cruz, *Bioprocess. Biosyst. Eng.* **2016**, *39 (2)*, 285–294. DOI: https://doi.org/10.1007/s00449-015-1512-6

[35] Z. Liu, X. Zheng, D. Liu, Y. Wang, C. Tao, *Chem. Eng. Process.* **2014**, *86*, 69–77. DOI: https://doi.org/10.1016/j.cep.2014.10.007

[36] D. Gu, Z. Liu, F. Qiu, J. Li, C. Tao, Y. Wang, *Adv. Powder Technol.* **2017**, *28 (10)*, 2514–2523. DOI: https://doi.org/10.1016/j.apt.2017.06.027

[37] D. Gu, Z. Liu, C. Xu, J. Li, C. Tao, Y. Wang, *Chem. Eng. Process.* **2017**, *118*, 37–46. DOI: https://doi.org/10.1016/j.cep.2017.04.018

[38] N. Ghobadi, C. Ogino, N. Ohmurab, *Open Chem. Eng. J.* **2016**, *10*, 88–109. DOI: https://doi.org/10.2174/1874123101610010088

[39] N. Ghobadi, C. Ogino, K. Yamabe, N. Ohmura, *J. Biosci. Bioeng.* **2017**, *123 (1)*, 101–108. DOI: https://doi.org/10.1016/j.jbiosc.2016.07.001

[40] A. Bakker, H. E. A. Van den Akker, in *Fluid Mixing IV, Institution of Chemical Engineers Symposium Series 121* (Ed: H. Benkreira), Taylor & Francis, London **1990**.

[41] C. A. Coulaloglou, L. L. Tavlarides, *Chem. Eng. Sci.* **1977**, *32 (11)*, 1289–1297. DOI: https://doi.org/10.1016/0009-2509(77)85023-9

[42] M. Kolano, M. Kraume, *Chem. Eng. Technol.* **2019**, *42 (8)*, 1670–1679. DOI: https://doi.org/10.1002/ceat.201900122

[43] M. Nishikawa, H. Kato, K. Hashimoto, *Ind. Eng. Chem. Process Des. Dev.* **1977**, *16 (1)*, 133–137. DOI: https://doi.org/10.1021/i260061a607

[44] M. O. Cerri, L. Futiwaki, C. D. F. Jesus, A. J. G. Cruz, A. C. Badino, *Biochem. Eng. J* **2008**, *39 (1)*, 51–57. DOI: https://doi.org/10.1016/j.bej.2007.08.009

[45] A. Campesi, M. O. Cerri, C. O. Hokka, A. C. Badino, *Bioprocess. Biosyst. Eng.* **2009**, *32 (2)*, 241–248. DOI: https://doi.org/10.1007/s00449-008-0242-4

[46] F. R. Schmidt, *Appl. Microbiol. Biotechnol.* **2005**, *68 (4)*, 425–435. DOI: https://doi.org/10.1007/s00253-005-0003-0

[47] D. C. Hempel, in *Jahrbuch Biotechnologie 1986/87*, Carl Hanser Verlag, München **1986**.

[48] P. R. Gogate, A. A. C. M. Beenackers, A. B. Pandit, *Biochem. Eng. J* **2000**, *6 (2)*, 109–144. DOI: https://doi.org/10.1016/S1369-703X(00)00081-4

[49] B. Letellier, C. Xuereb, P. Swaels, P. Hobbes, J. Bertrand, *Chem. Eng. Sci.* **2002**, *57 (21)*, 4617–4632. DOI: https://doi.org/10.1016/S0009-2509(02)00371-8

[50] G. Zhou, S. M. Kresta, *Chem. Eng. Sci.* **1998**, *53 (11)*, 2063–2079. DOI: https://doi.org/10.1016/S0009-2509(97)00438-7

[51] M. Wille, G. Langer, U. Werner, *Chem. Eng. Technol.* **2001**, *24 (5)*, 475–479. DOI: https://doi.org/10.1002/1521-4125(200105)24:5<475:AID-CEAT475>3.0.CO;2-L

[52] M. Stieß, *Mechanische Verfahrenstechnik – Partikeltechnologie 1*, Springer, Berlin **2009**.

[53] R. Polke, M. Schäfer, N. Scholz, in *Handbuch der Mechanischen Verfahrenstechnik*, John Wiley & Sons, Hoboken, NJ **2005**.

[54] T. Wucherpfennig, T. Hestler, R. Krull, *Microb. Cell Fact.* **2011**, *10 (85)*. DOI: https://doi.org/10.1186/1475-2859-10-58

[55] M. Kraume, A. Gäbler, K. Schulze, *Chem. Eng. Technol.* **2004**, *27 (3)*, 330–334. DOI: https://doi.org/10.1002/ceat.200402006

[56] J. Ritter, *PhD Thesis*, Technische Universität Berlin **2002**.

[57] A. Daub, M. Böhm, S. Delueg, M. Mühlmann, G. Schneider, J. Büchs, *J. Bio. Eng.* **2014**, *8*, 17. DOI: https://doi.org/10.1186/1754-1611-8-17

[58] A. Biedermann, H.-J. Henzler, *Chem. Ing. Tech.* **1994**, *66 (2)*, 209–211. DOI: https://doi.org/10.1002/cite.330660216

[59] A. W. Pacek, S. Chamsart, A. W. Nienow, A. Bakker, *Chem. Eng. Sci.* **1999**, *54 (19)*, 4211–4222. DOI: https://doi.org/10.1016/S0009-2509(99)00156-6

[60] S. Wollny, *PhD Thesis*, Technische Universität Berlin **2010**.

[61] R. Grenville, J. Giacomelli, D. Brown, G. Padron, *Chem. Eng.* **2017**, *124*, 42–50.

[62] A. Gabriele, A. W. Nienow, M. J. H. Simmons, *Chem. Eng. Sci.* **2009**, *64 (1)*, 126–143. DOI: https://doi.org/10.1016/j.ces.2008.09.018

[63] W. J. McManamey, *Chem. Eng. Sci.* **1979**, *34 (3)*, 432–434. DOI: https://doi.org/10.1016/0009-2509(79)85081-2

[64] A. W. Nienow, *Chem. Eng. Sci.* **1997**, *52 (15)*, 2557–2565. DOI: https://doi.org/10.1016/S0009-2509(97)00072-9

[65] J. A. Rocha-Valadez, E. Galindo, L. Serrano-Carreón, *J. Biotechnol.* **2007**, *130 (4)*, 394–401. DOI: https://doi.org/10.1016/j.jbiotec.2007.05.001

[66] J. C. van Suijdam, B. Metz, *Biotechnol. Bioeng.* **1981**, *23 (1)*, 111–148. DOI: https://doi.org/10.1002/bit.260230109

[67] M. Reuß, *Chem. Eng. Technol.* **1988**, *11 (1)*, 178–187. DOI: https://doi.org/10.1002/ceat.270110124

[68] H. Weit, J. Schwedes, *Chem. Ing. Tech.* **1986**, *58 (10)*, 818–819. DOI: https://doi.org/10.1002/cite.330581015

[69] K. Van't Riet, J. Tramper, *Basic bioreactor design*, CRC Press, Boca Raton, FL **1991**.

[70] J. J. Smith, M. D. Lilly, R. I. Fox, *Biotechnol. Bioeng.* **1990**, *35 (10)*, 1011–1023. DOI: https://doi.org/10.1002/bit.260351009

[71] H. Y. Makagiansar, P. Ayazi Shamlou, C. R. Thomas, M. D. Lilly, *Bioprocess. Biosyst. Eng.* **1993**, *9 (2)*, 83–90. DOI: https://doi.org/10.1007/BF00369035

[72] P. Jüsten, G. C. Paul, A. W. Nienow, C. R. Thomas, *Biotechnol. Bioeng.* **1998**, *59 (6)*, 762–775. DOI: https://doi.org/10.1002/(SICI)1097-0290(19980920)59:6<762:AID-BIT13>3.0.CO;2-7

[73] Y. Liu, Z.-J. Wang, J.-Y. Xia, C. Haringa, Y.-P. Liu, J. Chu, Y.-P. Zhuang, S.-L. Zhang, *Biochem. Eng. J* **2016**, *114*, 209–217. DOI: https://doi.org/10.1016/j.bej.2016.07.006

[74] A. Amanullah, P. Jüsten, A. Davies, G. C. Paul, A. W. Nienow, C. R. Thomas, *Biochem. Eng. J* **2000**, *5 (2)*, 109–114. DOI: https://doi.org/10.1016/S1369-703X(99)00059-5

[75] Z. J. Li, V. Shukla, K. S. Wenger, A. P. Fordyce, A. G. Pedersen, M. R. Marten, *Biotechnol. Prog.* **2002**, *18 (3)*, 437–444. DOI: https://doi.org/10.1021/bp020023c

[76] J. L. Casas López, J. A. Sánchez Pérez, J. M. Fernández Sevilla, F. G. Acién Fernández, E. Molina Grima, Y. Chisti, *J. Chem. Technol. Biotechnol.* **2004**, *79 (10)*, 1119–1126. DOI: https://doi.org/10.1002/jctb.1100

[77] J. A. Rocha-Valadez, M. Hassan, G. Corkidi, C. Flores, E. Galindo, L. Serrano-Carreón, *Biotechnol. Bioeng.* **2005**, *91 (1)*, 54–61. DOI: https://doi.org/10.1002/bit.20489

[78] K. C. Lee, M. Yianneskis, *AIChE J.* **1998**, *44 (1)*, 13–24. DOI: https://doi.org/10.1002/aic.690440104

[79] L. Hohl, R. P. Panckow, J. M. Schulz, N. Jurtz, L. Böhm, M. Kraume, *Chem. Ing. Tech.* **2018**, *90 (11)*, 1709–1726. DOI: https://doi.org/10.1002/cite.201800079
[80] J. J. J. Gillissen, H. E. A. Van den Akker, *AIChE J.* **2012**, *58 (12)*, 3878–3890. DOI: https://doi.org/10.1002/aic.13762
[81] A. Rosseburg, J. Fitschen, J. Wutz, T. Wucherpfennig, M. Schlüter, *Chem. Eng. Sci.* **2018**, *188*, 208–220. DOI: https://doi.org/10.1016/j.ces.2018.05.008
[82] F. Guillard, C. Trägårdh, *Chem. Eng. Technol.* **1999**, *22 (3)*, 187–195. DOI: https://doi.org/10.1002/(SICI)1521-4125(199903)22:3<187:AID-CEAT187>3.0.CO;2-9
[83] F. Guillard, C. Trägårdh, L. Fuchs, *Chem. Eng. Sci.* **2000**, *55 (23)*, 5657–5670. DOI: https://doi.org/10.1016/S0009-2509(00)00201-3

